Dihydrogen Bond-Interaction-Induced Separation of Hexane Isomers by Self-Assembled Carborane Metallacycles

Peng-Fei Cui[1], Yue-Jian Lin[1], Zhen-Hua Li[1], Guo-Xin Jin[1]*

[1.]Shanghai Key Laboratory of Molecular Catalysis and Innovative Materials, Collaborative Innovation Center of Chemistry for Energy Materials, Department of Chemistry, Fudan University, Shanghai 200433, P. R. China.

*E-mail: gxjin@fudan.edu.cn.

Contents

1. Experimental details

1.1 Materials:

All reagents and solvents were purchased from commercial sources (Sigma Aldrich and Adamas-beta) and used as supplied unless otherwise mentioned. The starting material $[Cp^*IrCl_2]_2$ [1] (Cp^*= η^5-pentamethylcyclopentadienyl) was prepared by literature method.

1.2 Methods:

NMR spectra were recorded on Bruker AVANCE I 400 and VANCE-DMX 500 Spectrometers. Spectra were recorded at room temperature and referenced to the residual protonated solvent for NMR spectra. Proton chemical shift (δH = 7.26 ($CDCl_3$)) and (δC = 77.16 ($CDCl_3$)); and ((δ H = 3.31 (CD_3OD)) are reported relative to the solvent residual peak. Coupling constants are expressed in hertz. Elemental analyses were performed on an Elementar Vario EL III analyzer. IR spectra of the solid samples (KBr tablets) in the range 400-4000 cm^{-1} were recorded on a Nicolet AVATAR-360IR spectrometer. ESI-MS spectra were recorded on a Micro TOF II mass spectrometer using electrospray ionization.

Thermogravimetric (TGA) analysis was carried out using a Q5000IR analyzer (TA Instruments) with an automated vertical overhead thermobalance. The samples were heated at the rate of 10 °C/min using N_2 as the protective gas. Before measurements, the solids were blown under N_2 at 10ml/min for 30 min to remove the surface-physically adsorbed molecules.

Intelligent Gravimetric Analyser (IGA) analysis was carried out using an IGA100B instrument with an automated vertical thermobalance. Samples were analyzed at 25 °C with the P/P_0 = 0.05, 0.10, 0.15, 0.20, 0.25, 0.30, 0.35…0.90, 0.95.

Gas chromatography (GC) analysis: GC measurements were carried out using a PE680-ST8 instrument configured with an FID detector and a DB-624 column (30 m × 0.53 mm × 3.0 μm). Samples were analyzed using headspace injections and were performed by incubating the sample at 70 °C for 10 minutes followed by sampling 1 mL of the headspace. The relative uptakes of hexane

isomers in complex **3a** were measured by heating to release the adsorbed vapor and detecting the relative amounts of isomers in the released vapor using gas chromatography. Before measurements, the solids were blown under N_2 at 10ml/min for 30 min to remove the surface-physically adsorbed molecules.

1.3 Synthetic Procedures:

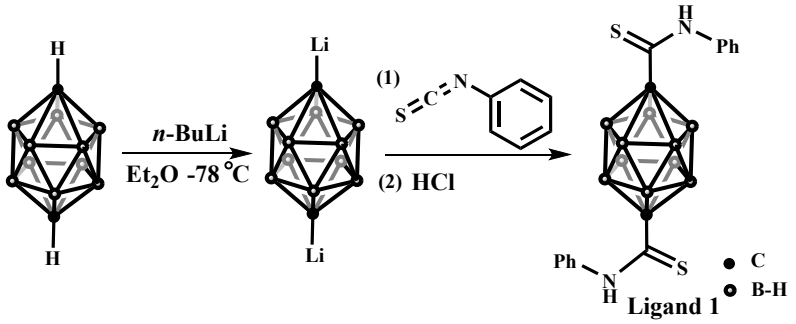

Scheme S1. Synthesis of **Ligand 1**.

synthesis of Ligand 1. A suspension of *n*-BuLi (1.6 mol/L in *n*-hexane, 1.3 ml, 2.0 mmol) was added to a solution of *p*-carborane (144 mg, 1 mmol) in ether 10 ml at -78 °C over a period of 1 h, then Phenyl isothiocyanate (2 ml) was added at room temperature and the resulting mixture was stirred for 24 h. The reaction mixture was quenched with dilute HCl and the organic phase was separated and the water phase extracted with diethyl ether (3 × 10 mL). The solvent was then removed under vacuo and the residue was purified by column chromatography on silica gel. Elution with petroleum ether gave Ligand **1** as a yellow solid (yield: 320 mg, 78%). ^{1}H NMR (400 MHz; $CDCl_3$, ppm): δ = 2.43-3.50 (br, 10H, B-H); 7.28 (t, J = 7.2 Hz, 2H, Ar-H); 7.39 (t, J = 8.0 Hz, 4H, Ar-H); 7.46 (d, J = 8.0 Hz, 4H, Ar-H); 8.70 (s, 2H, N-H). ^{13}C{^{1}H} NMR (101 MHz; $CDCl_3$, ppm): δ = 88.87 (cage C); 124.10, 127.82, 129.25, 138.39 (Ar-C); 188.07 (N-C=S). ^{11}B NMR (160 MHz, $CDCl_3$, ppm): δ = -12.97, -14.03. IR (KBr disk, cm^{-1}): v = 693, 752, 1029, 1358, 1497, 1645, 2561, 3437 cm^{-1}. Calcd for Ligand **1** : $C_{16}H_{22}B_{10}N_2S_2$: C, 46.35; H, 5.35, N, 6.76. Found: C, 46.03; H, 5.52; N, 6.44. ESI-MS: m/z = 416.2298 (calcd for $[M + H]^+$ 416.2268).

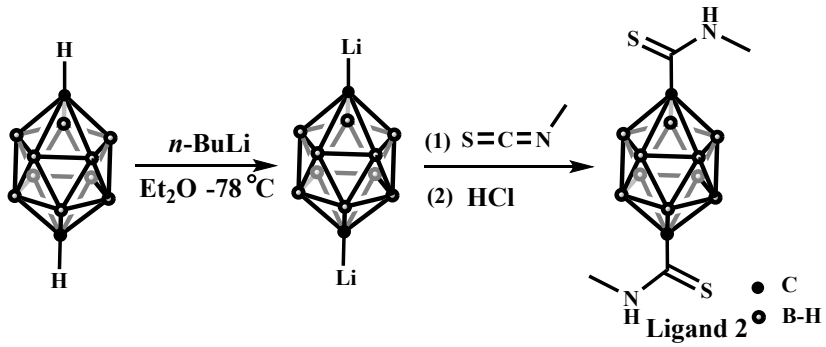

Scheme S2. Synthesis of **Ligand 2**.

Synthesis of Ligand 2. A suspension of *n*-BuLi (1.6 mol/L in *n*-hexane, 1.3 ml, 2.0 mmol) was added to a solution of *p*-carborane (144 mg, 1 mmol) in ether 10 ml at -78 °C over a period of 1 h, then methyl isothiocyanate (150 mg, 2 mmol) was added at room temperature and the resulting mixture was stirred for 24 h. The reaction mixture was quenched with dilute HCl and the organic phase was separated and the water phase extracted with diethyl ether (3 × 10 mL). The solvent was then removed under vacuo and the residue was purified by column chromatography on silica gel. Elution with petroleum ether gave Ligand **2** as a light yellow solid (yield: 230 mg, 79%). ^{1}H NMR (400 MHz; $CDCl_3$, ppm): δ = 1.63-2.84 (br, 10H, B-H); 3.04, 3.05 (s, 6H, CH_3); 7.41 (s, 2H, N-H). $^{13}C\{^{1}H\}$ NMR (101 MHz; $CDCl_3$, ppm): δ = 35.04 (CH_3); 81.69 (cage C); 189.28 (N-C=S). ^{11}B NMR (160 MHz, $CDCl_3$, ppm): δ = -12.59, -13.13, -14.18, -14.82, -15.59. IR (KBr disk, cm^{-1}): ν = 695, 754, 1023, 1495, 2559, 3427 cm^{-1}. Calcd for Ligand **2**: $C_6H_{18}B_{10}N_2S_2$: C, 24.81; H, 6.25, N, 9.65. Found: C, 24.50; H, 6.52; N, 9.44. ESI-MS: m/z = 291.1980 (calcd for $[M + H]^+$ 291.1991).

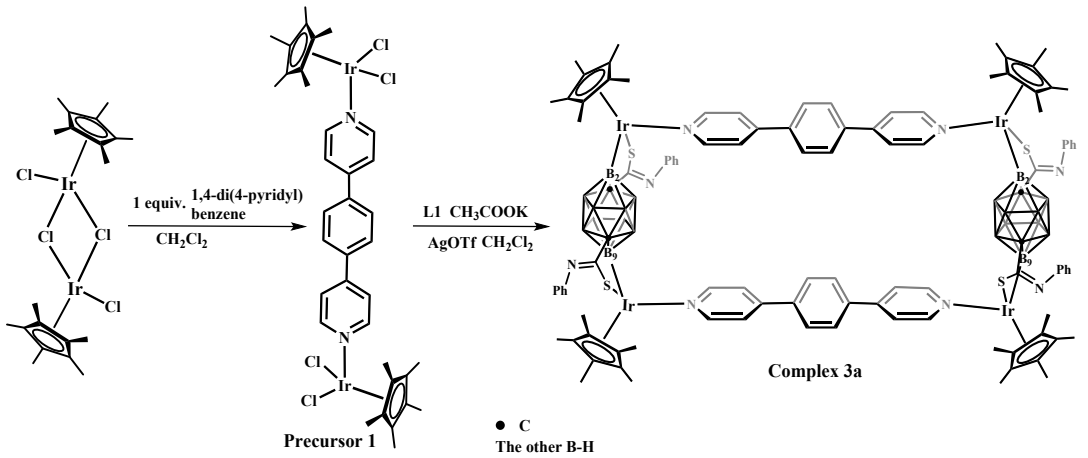

Scheme S3. Synthesis of complex **3a**.

Synthesis of complex 3a. Precursor 1: $[Cp^*IrCl_2]_2$ (80 mg, 0.1 mmol), 1,4-di(4-pyridyl) benzene (23.2 mg, 0.1mmol) and AgOTf (102 mg, 0.4 mmol) were added in CH_2Cl_2 (10 ml) stirring for 10h. Then potassium acetate (10 mg) and the ligand **1** (40.4 mg, 0.1 mmol) were added to the mixture at room temperature. The reaction mixture was stirred for another 24h then filtered. The filtrate was concentrated and further purified via neutral alumina gel chromatography (CH_2Cl_2: CH_3OH, 50: 1). Red solids were obtained and dried under vacuo to give the complex **3a**: 138 mg 82%. ^1H NMR (400 MHz; $CDCl_3$, ppm): δ = 1.65 (s, 60H, Cp*-H); 1.68-3.38 (br, 16H, B-H); 6.87 (d, 8H, J = 7.2 Hz, Ar-H); 7.00 (t, 4H, J = 7.6 Hz, Ar-H); 7.29 (t, 8H, J = 7.6 Hz, Ar-H); 7.34 (d, J = 8.0 Hz, 4H, Ar-H); 7.41 (d, J = 7.6 Hz, 4H, Ar-H); 7.54 (d, J = 8.0 Hz, 8H, pyrazine-H); 8.75 (d, J = 8.0 Hz, 8H, pyrazine-H). ^{11}B NMR (160 MHz, $CDCl_3$, ppm): δ = -13.12. IR (KBr disk, cm^{-1}): ν = 814, 1028, 1093, 1156, 1265, 1443, 1485, 1525, 1638, 1715, 2192, 2580, 2850, 2967 cm^{-1}. Anal. Calcd for complex **3a**: $C_{104}H_{120}B_{20}Ir_4N_8S_4$: C, 48.13; H, 4.66; N, 4.32. Found: C, 48.47; H, 4.42; N, 4.31.

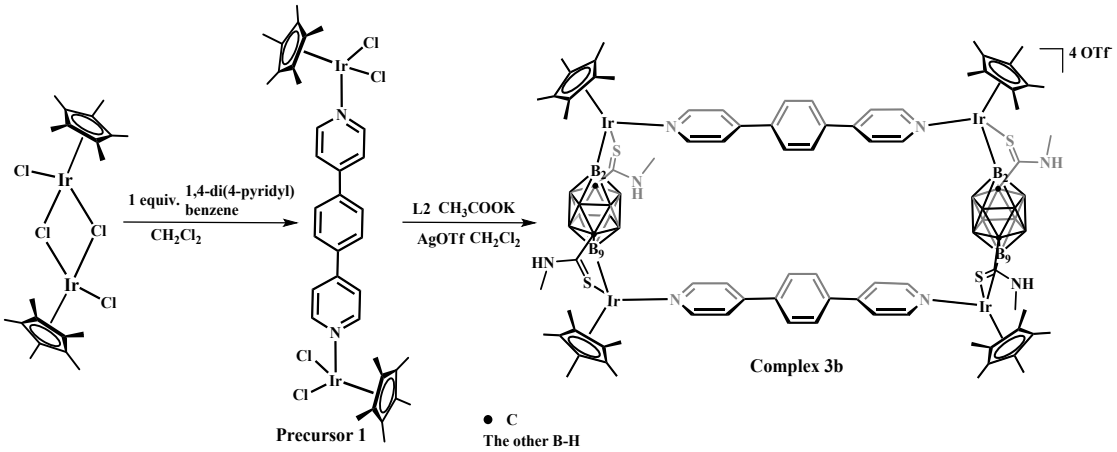

Scheme S4. Synthesis of complex **3b**.

Synthesis of complex 3b. The ligand **2** (29.0 mg, 0.1 mmol), potassium acetate (10 mg) and AgOTf (102 mg, 0.4 mmol) were added to the **precursor 1** at room temperature. The reaction mixture was stirred for another 24h then filtered. The filtrate was concentrated and further purified via neutral alumina gel chromatography (CH_2Cl_2: CH_3OH, 50: 1). Yellow solids were obtained and dried under vacuo to give the complex **3b**: 123 mg 85%. ^1H NMR (400 MHz; $CDCl_3$, ppm): δ = 1.78-2.63 (br, 16H, B-H); 1.71 (s, 60H, Cp*-H); 3.24 (s, 12H, CH_3); 7.40 (d, J = 5.2 Hz, 4H, Py-H); 7.68 (d, J = 5.2 Hz, 4H, Py-H); 8.37 (d, 4H, J = 5.0 Hz, Py-H); 8.97 (d, 4H, J = 5.0 Hz, Py-H); 9.77 (s, 4H, N-H); 7.75 (s, 8H, Ph-H). ^{19}F NMR (376 MHz, $CDCl_3$, ppm): δ = 78.77. ^{11}B NMR (160 MHz, $CDCl_3$, ppm): δ = -12.01. IR (KBr disk, cm^{-1}): ν = 817, 1025, 1090, 1153, 1268, 1441, 1483, 1584, 1634, 1773, 2575, 3245 cm^{-1}. Anal. Calcd for complex **3b**: C_{86} H_{116} B_{20} Ir_4 N_8 S_8 O_{12} F_{12}: C, 35.33; H, 4.00; N, 3,83. Found: C, 35.20; H, 3.79; N, 4.11.

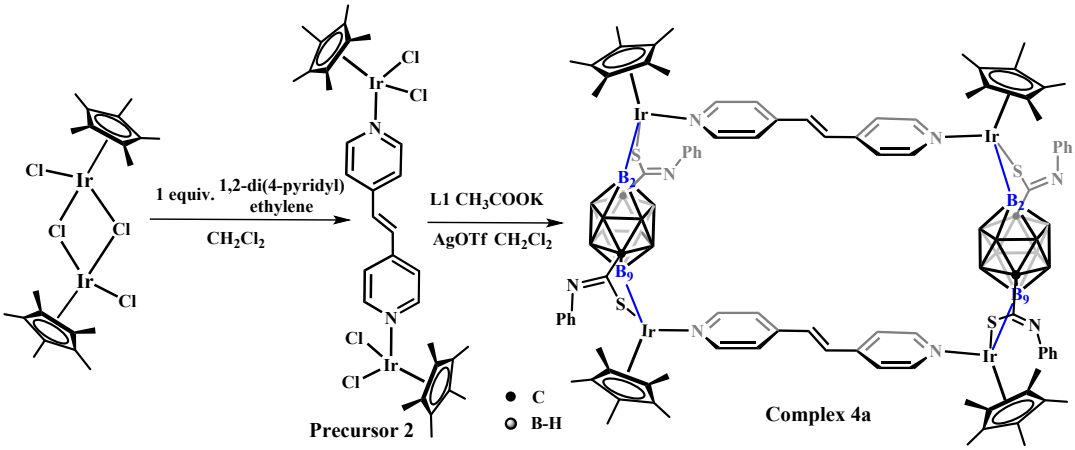

Scheme S5. Synthesize of complex **4a**.

Synthesis of complex 4a. Precursor 2: $[Cp^*IrCl_2]_2$ (80 mg, 0.1 mmol), 1,2di(4-pyridyl) ethylene (18.3 mg, 0.1mmol) and AgOTf (102 mg, 0.4 mmol) were added in CH_2Cl_2 (10 ml) stirring for 10h. Then the ligand **1** (40.4 mg, 0.1 mmol) and potassium acetate (10 mg) were added to the **precursor 2** in dark at room temperature. The reaction mixture was stirred for another 24h then filtered. The filtrate was concentrated and further purified via neutral alumina gel chromatography (CH_2Cl_2: CH_3OH, 50: 1). Red solid were obtained and dried under vacuo to give the complex **4a**: 99.8 mg 79%. ^1H NMR (400 MHz; $CDCl_3$, ppm): δ = 1.95-2.88 (br, 16H, B-H); 1.61 (s, 60H, Cp*-H); 6.89 (d, 8H, Ar-H); 7.12 (t, 4H, Ar-H); 7.17 (t, 8H, Ar-H); 7.19 (s, 8H, ethylene-H); 7.26 (8H, pyrazine-H); 8,80,8.86 (8H, pyrazine-H). ^{11}B NMR (160 MHz, $CDCl_3$, ppm): δ = -12.74. IR (KBr disk, cm^{-1}): ν = 814, 1028, 1095, 1153, 1261, 1442, 1485, 1524, 1593, 1635, 1670, 1712, 2585, 2850, 2961 cm^{-1}. Anal. Calcd for complex **4a:** $C_{96}H_{116}B_{20}Ir_4N_8S_4$: C, 46.21; H, 4.69; N, 4.49. Found: C, 46.01; H, 4.95; N, 4.16.

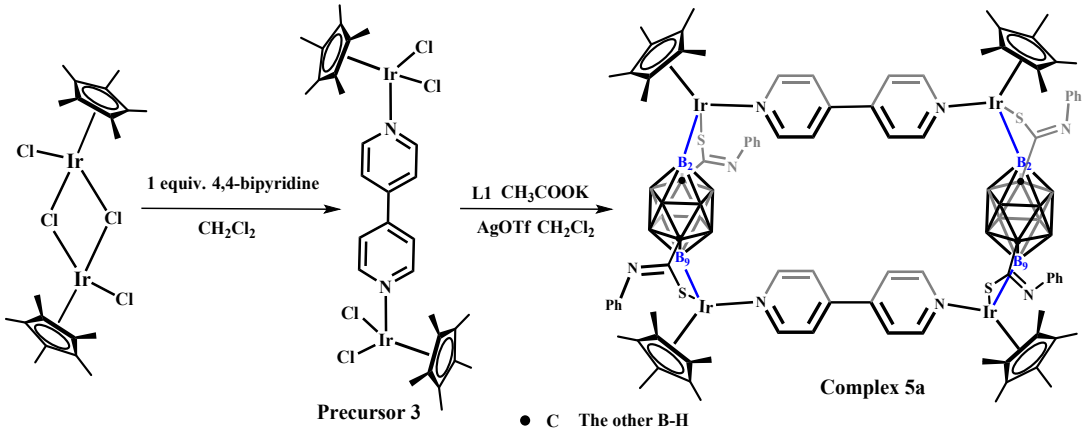

Scheme S6. Synthesize of complex **5a**.

Synthesis of complex 5a. Precursor 3: $[Cp^*IrCl_2]_2$ (80 mg, 0.1 mmol), 4,4'-bipyridine (15.6 mg, 0.1mmol) and AgOTf (102 mg, 0.4 mmol) were added in CH_2Cl_2 (10 ml) stirring for 10h. Then the ligand **1** (40.4 mg, 0.1 mmol) and potassium acetate (10 mg) were added to the **precursor 3** in dark at room temperature. The reaction mixture was stirred for another 24h then filtered. The filtrate was concentrated and further purified via neutral alumina gel chromatography (CH_2Cl_2: CH_3OH, 50: 1). Red solids were obtained and dried under vacuo to give the complex **5a**: 96.3 mg 80%. ^1H NMR (400 MHz; $CDCl_3$, ppm): δ = 1.94-2.87 (br, 16H, B-H); 1.61 (s, 60H, Cp*-H); 6.83 (d, 8H, J = 7.4 Hz, Ar-H); 7.0 (t, J = 7.0 Hz, 4H, Ar-H); 7.30 (t, J = 7.4 Hz, 8H, Ar-H); 7.35 (d, 8H, pyrazine-H); 8.97 (d, 8H, pyrazine-H). ^{11}B NMR (160 MHz, $CDCl_3$, ppm): δ = -12.57. IR (KBr disk, cm^{-1}): ν = 814, 1028, 1095, 1153, 1261, 1442, 1485, 1524, 1593, 1635, 1712, 2585, 2850, 2961 cm^{-1}. Anal. Calcd for complex **5a**: $C_{92}H_{112}B_{20}Ir_4N_8S_4$: C, 45.23; H, 4.62; N, 4.59. Found: C, 45.03; H, 4.94; N, 4.19.

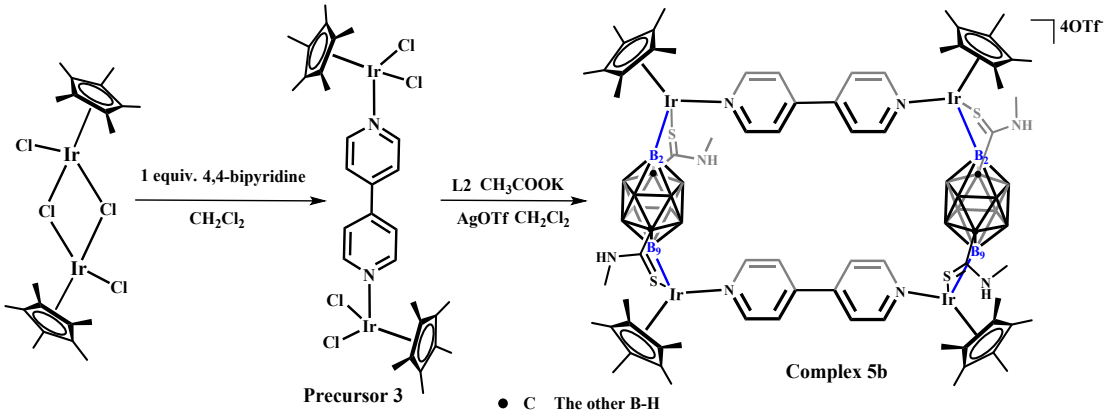

Scheme S7. Synthesize of complex **5b**.

Synthesis of complex 5b. The ligand **2** (29.2 mg, 0.1 mmol) and potassium acetate (10 mg) were added to the **precursor 3** in dark at room temperature. The reaction mixture was stirred for another 24h then filtered. The filtrate was concentrated and further purified via neutral alumina gel chromatography (CH_2Cl_2: CH_3OH, 50: 1). Red solids were obtained and dried under vacuo to give the complex **5b**: 104.8 mg 75%. ^{1}H NMR (400 MHz; $CDCl_3$, ppm): δ = 1.78-2.04 (br, 16H, B-H); 1.72 (s, 60H, Cp*-H); 3.21 (d, 12H, J = 3.9 Hz, CH_3); 7.62 (d, 4H, J = 5.2 Hz, py-H); 7.82 (d, 4H, J = 5.2 Hz, py-H); 8.46 (d, 4H, J = 5.2 Hz, py-H); 9.12 (d, 4H, J = 5.2 Hz, py-H); 9.71 (s, 4H, NH). ^{19}F NMR (376 MHz, $CDCl_3$, ppm): δ = 78.13. ^{11}B NMR (160 MHz, $CDCl_3$, ppm): δ = -14.22. IR (KBr disk, cm^{-1}): ν = 814, 1028, 1095, 1153, 1261, 1442, 1485, 1524, 1593, 1635, 1712, 2585, 2850, 3421 cm^{-1}. Anal. Calcd for complex **5b**: C_{76} H_{108} B_{20} Ir_4 N_8 S_8 O_{12} F_{12}: C, 32.66; H, 3.89; N, 4.01. Found: C, 32.33; H, 3.94; N, 4.29.

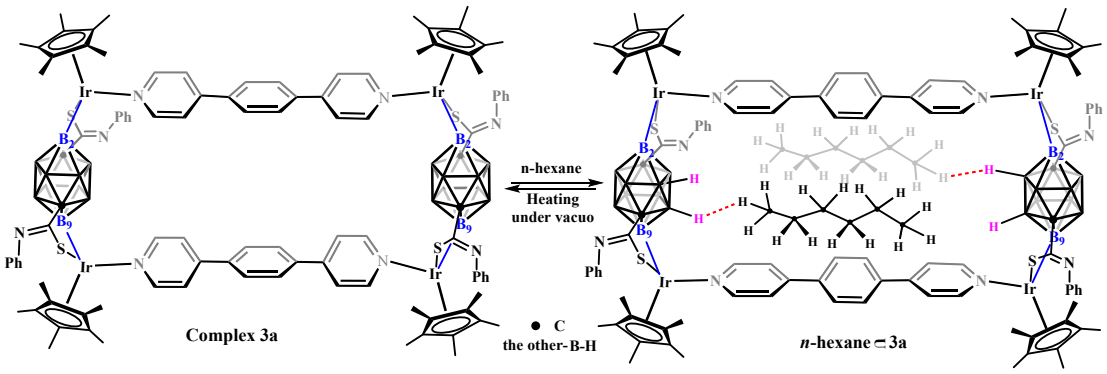

Scheme S8. Synthesize of complex ***n*-hexane⊂3a**.

Synthesis of complex *n*-hexane⊂3a. The complex **3a** was soaked in the *n*-hexane solution for one day. Then the solids were blown under N_2 for 30 mins. Red solids were obtained to give the complex ***n*-hexane⊂3a**. ^{1}H NMR (400 MHz; $CDCl_3$, ppm): δ = 0.88, 1.25 (m, 28H, *n*-hexane); δ = 1.82-2.20 (br, 16H, B-H); 1.67 (s, 60H, Cp*-H); 7.34 (m, 20H, Ph-Carborane); 7.56 (d, J = 3.7 Hz, 8H, Py-H); 8.70 (d, 8H, J = 2.7 Hz, Py-H); 7.77 (s, 8H, Ph-1,4-di(4-pyridyl) benzene). ^{11}B NMR (160 MHz, $CDCl_3$, ppm): δ = -9.95, -21.23, -52.70. IR (KBr disk, cm^{-1}): ν = 817, 1025, 1090, 1156, 1265, 1442, 1483, 1524, 1634, 1713, 2575, 2850, 2967 cm^{-1}.

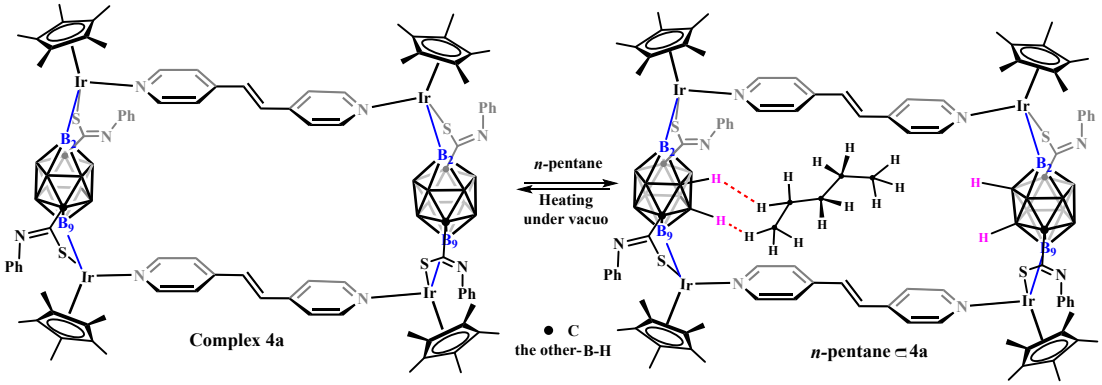

Scheme S9. Synthesize of complex ***n*-pentane⊂4a**.

Synthesis of complex *n*-pentane⊂4a. The complex **4a** was soaked in the *n*-pentane solution for one day. Then the solids were blown under N_2 for 30 mins. Dark red solids were obtained to give the complex ***n*-pentane⊂4a**. ^{1}H NMR (400 MHz; $CDCl_3$, ppm): δ = 0.92, 1.26 (m, 12H, *n*-pentane); 1.62 (s, 60H, Cp*-H); 6.98 (4H, Ph-H); 7.20 (8H, Ph-H); 7.25 (4H, enthylene-H) 7.07, 7.13 (d, 8H,

Py-H); 8.08, 8.64 (8H, Py-H). ^{11}B NMR (160 MHz, $CDCl_3$, ppm): δ = -9.95, -21.23, -52.70. IR (KBr disk, cm^{-1}): *v* = 814, 1027, 1096, 1152, 1261, 1442, 1485, 1524, 1594, 1636, 1673, 1712, 2585, 2850, 2961 cm^{-1}.

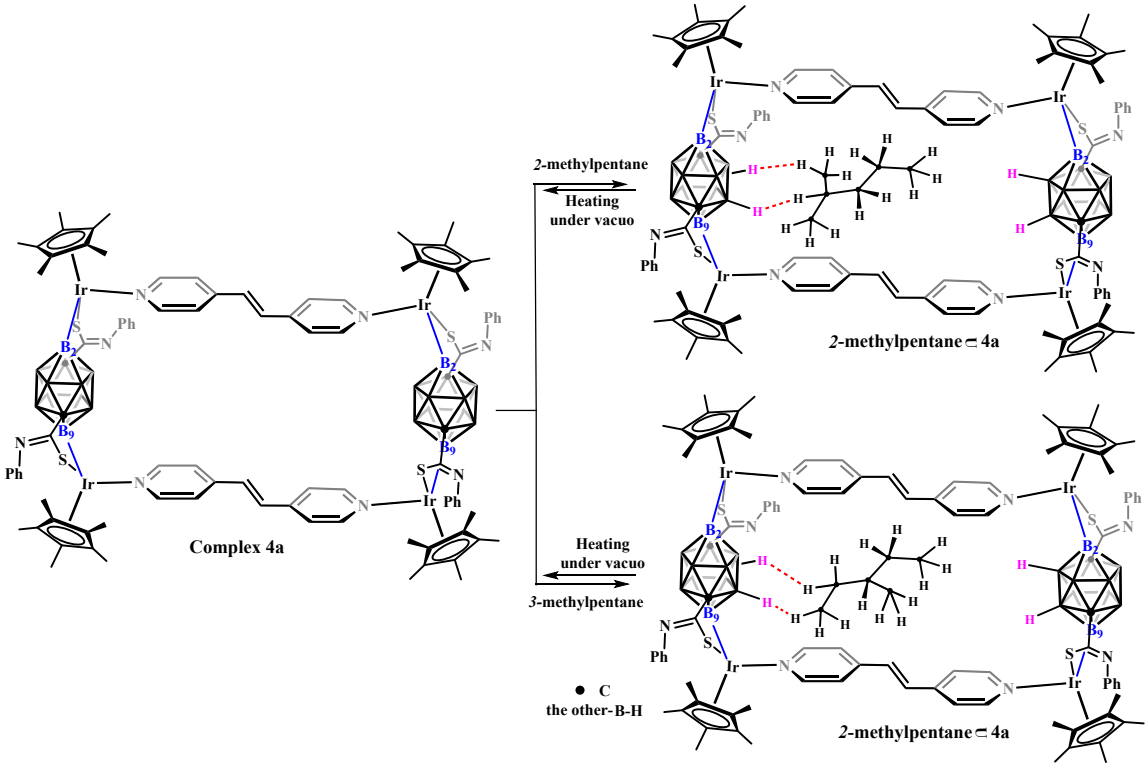

Scheme S10. Synthesize of complex ***2*-methylpentane⊂4a**.

Synthesis of complex *2*-methylpentane⊂4a. The complex **4a** was soaked in the *2*-methylpentane solution for one day. Then the solids were blown under N_2 for 30 mins. Dark red solids were obtained to give the complex ***2*-methylpentane⊂4a**. ^{1}H NMR (400 MHz; $CDCl_3$, ppm): *δ* = 0.88, 1.11, 1.26 (m, 14H, *2*-methylpentane); 1.61 (s, 60H, Cp*-H); 6.85 (d, *J* = 4.6 Hz, 8H, Ph-H); 6.99 (4H, Ph-H); 7.12 (8H, Ph-H); 7.16 (8H, Py-H) 7.28 (s, 4H, enthylene-H); 8.79, 8.89 (8H, Py-H). ^{11}B NMR (160 MHz, $CDCl_3$, ppm): δ = -0.51, -11.77. IR (KBr disk, cm^{-1}): *v* = 814, 1025, 1096, 1153, 1260, 1440, 1485, 1525, 1594, 1636, 1672, 1712, 2585, 2850, 2960 cm^{-1}.

Synthesis of complex *3*-methylpentane⊂4a. The complex **4a** was soaked in the *3*-methylpentane solution for one day. Then the solids were blown under N_2 for 30 mins. Dark red solids were obtained to give the complex ***3*-methylpentane⊂4a**. ^{1}H NMR (400 MHz; $CDCl_3$, ppm): *δ* = 0.85,

0.99, 1.25, 1.33 (*3*-methylpentane); 1.61 (s, 60H, Cp*-H); 6.87 (d, J = 4.4 Hz, 8H, Ph-H); 6.99 (4H, Ph-H); 7.12 (8H, Ph-H); 7.17 (8H, Py-H) 7.28 (s, 4H, enthylene-H); 8.81, 8.90 (8H, Py-H).

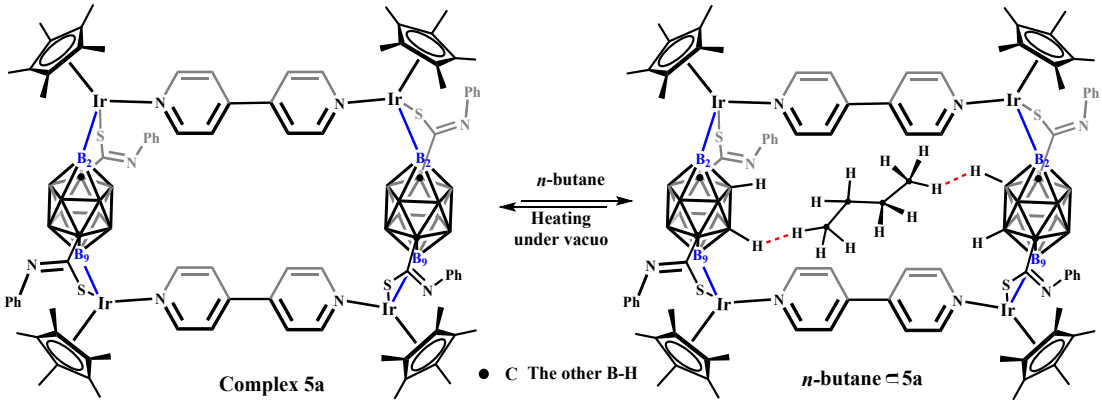

Scheme S11. Synthesize of complex ***n*-butane⊂5a**.

Synthesis of complex *n*-butane⊂5a. The gas of *n*-butane was passed in the solution of complex **5a** solution in CH_2Cl_2. One day later, the solution was evaporated. Then the solids were blown under N_2 for 30 mins. Yellow solids were obtained to give the complex ***n*-butane⊂5a**. ^{1}H NMR (400 MHz; $CDCl_3$, ppm): δ = 0.88, 1.27 (m, *n*-butane); 1.67 (s, 60H, Cp*-H); 6.85 (4H, Ph-H); 7.01 (8H, Ph-H); 7.31 (8H, Ph-H); 7.45, 7.53 (8H, Py-H). ^{11}B NMR (160 MHz, $CDCl_3$, ppm): δ = -4.91, -11.65, -19.11. IR (KBr disk, cm^{-1}): ν = 814, 1027, 1096, 1150, 1260, 1443, 1485, 1525, 1595, 1636, 1713, 2585, 2850, 2960 cm^{-1}.

NMR Data:

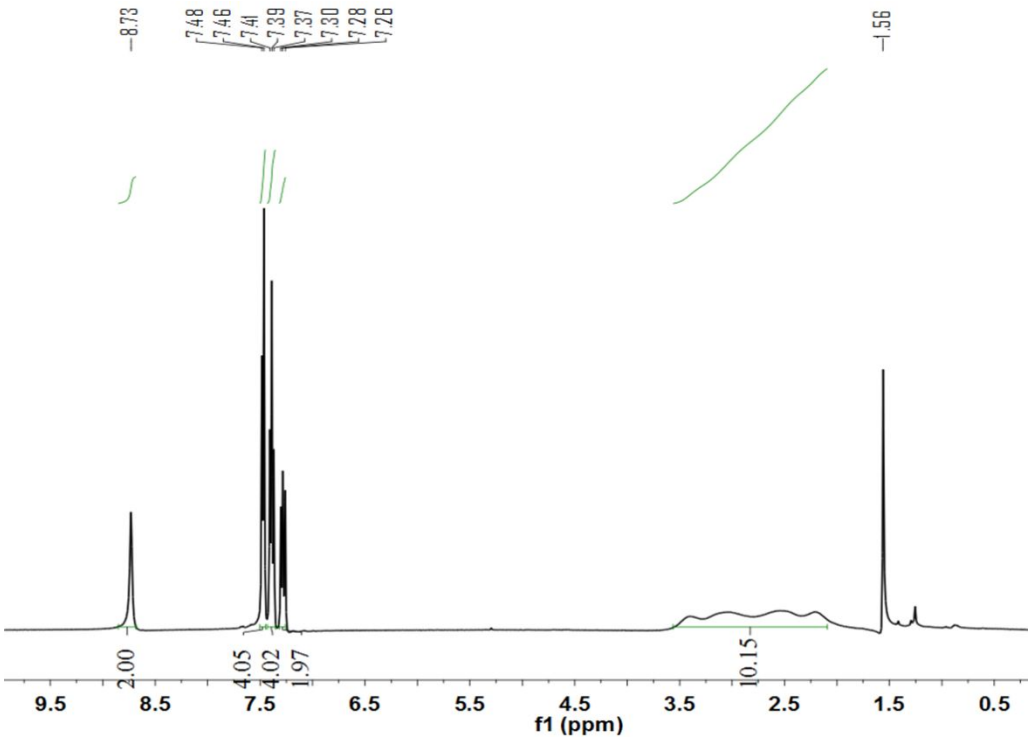

Figure S1. ^{1}H NMR (400 Hz, $CDCl_3$, ppm) of **L1**.

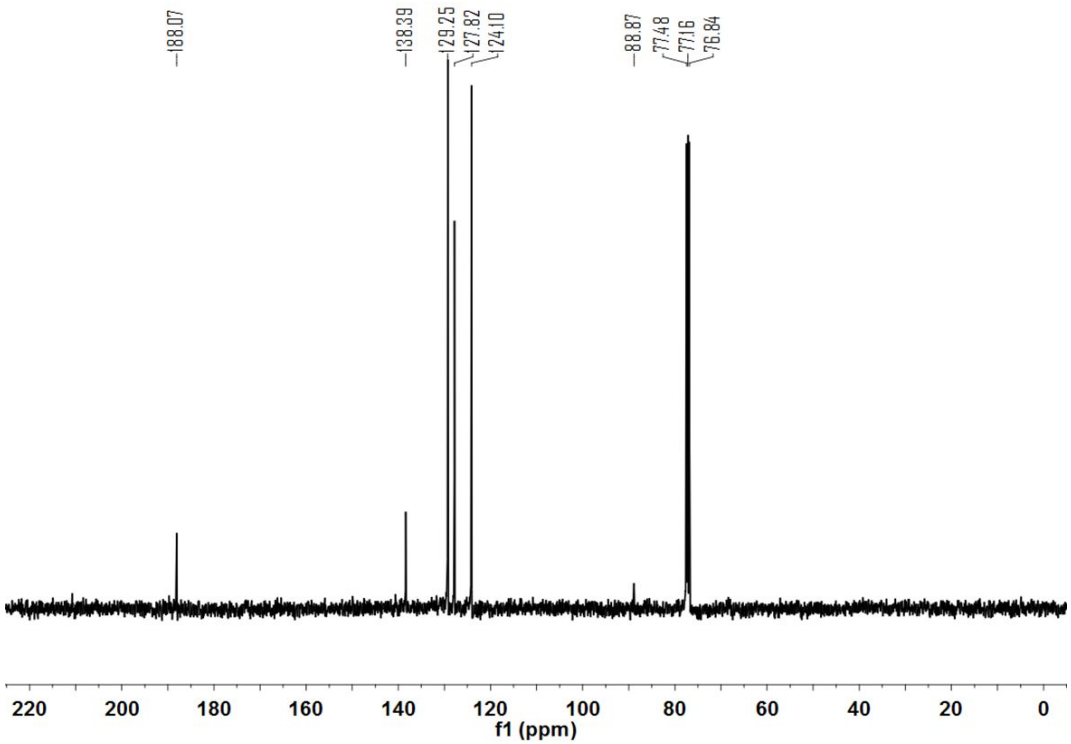

Figure S2. $^{13}C\{^{1}H\}$ NMR (101 MHz, $CDCl_3$, ppm) of **L1**.

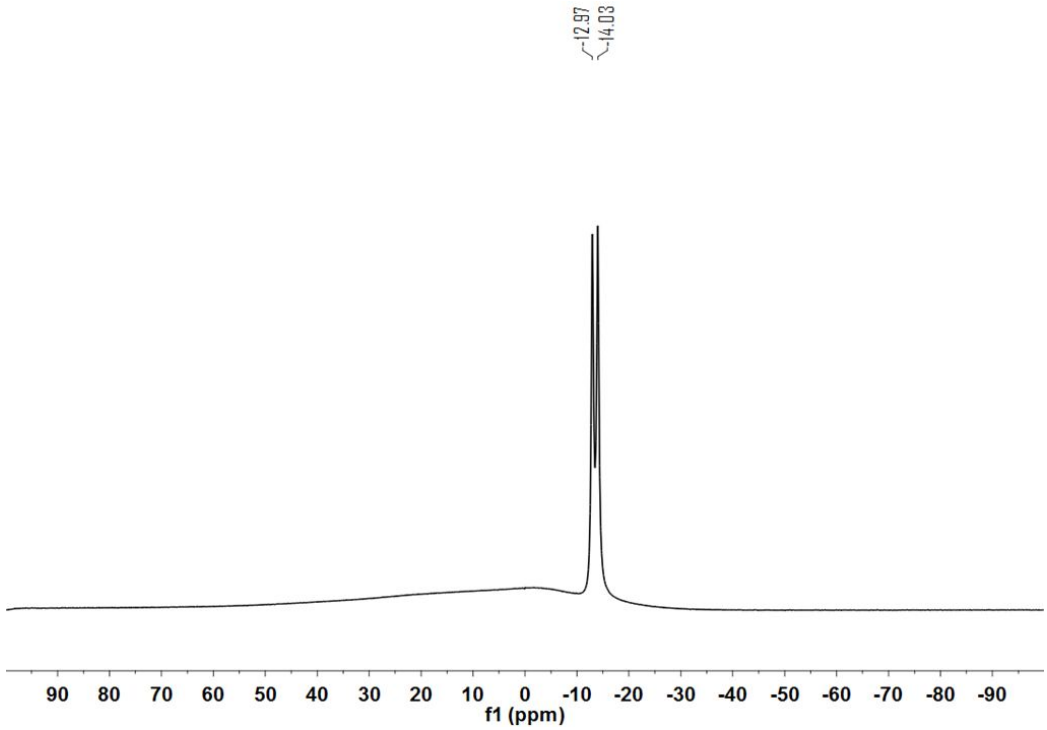

Figure S3. ^{11}B NMR (160 MHz, $CDCl_3$, ppm) of **L1**.

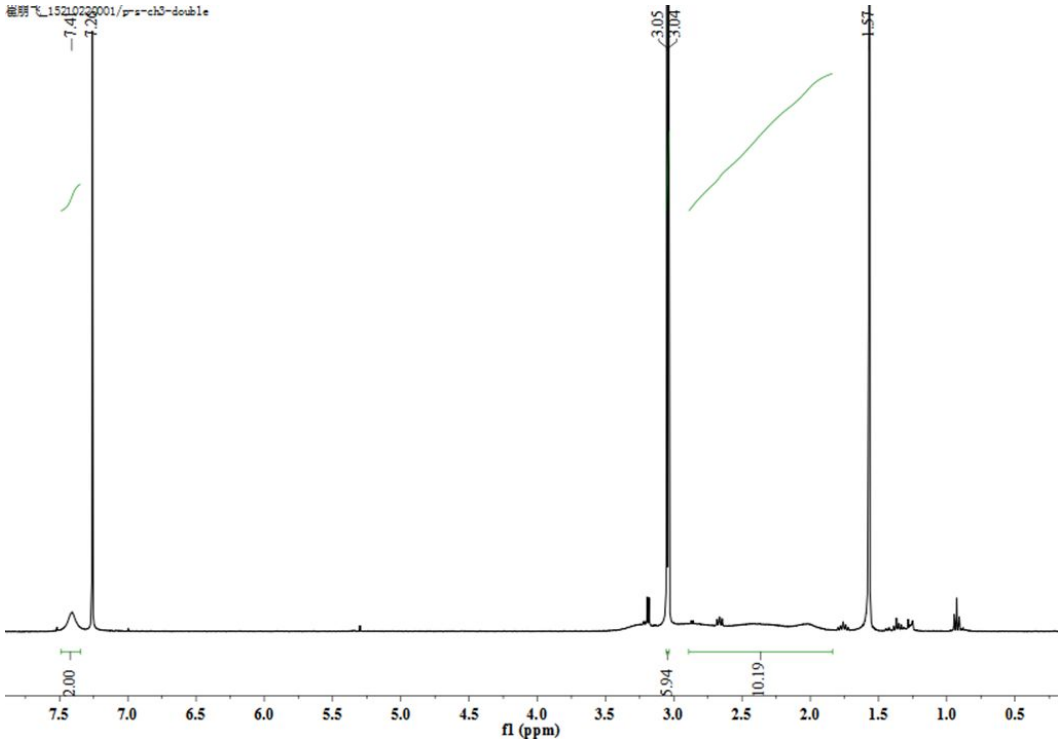

Figure S4. ^{1}H NMR (400 Hz, $CDCl_3$, ppm) of **L2**.

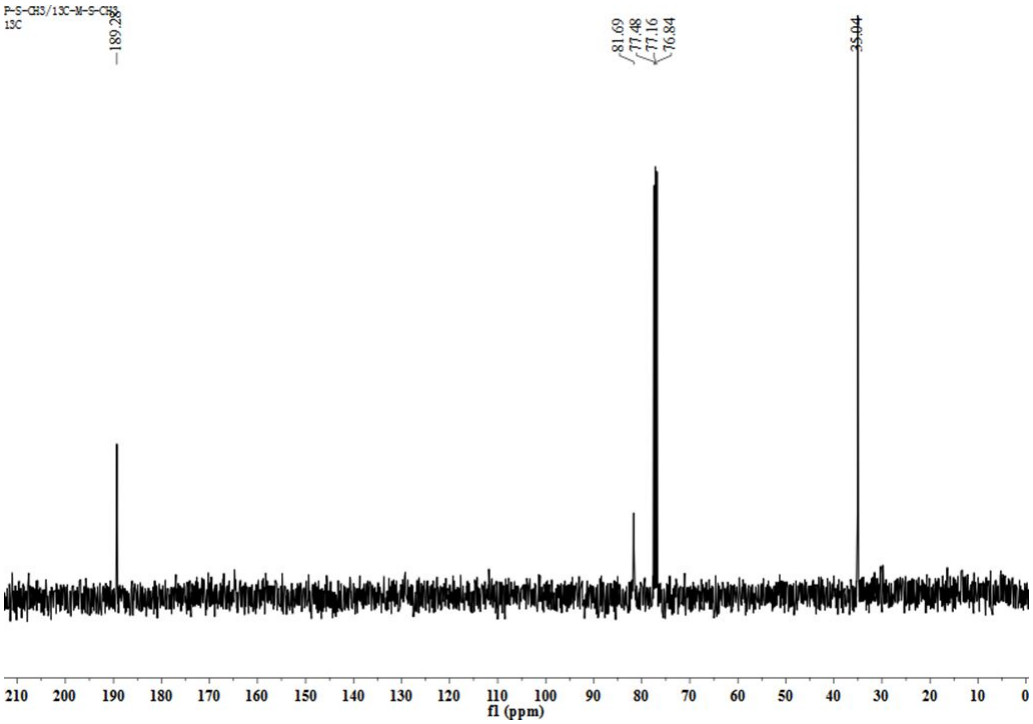

Figure S5. $^{13}C\{^{1}H\}$ NMR (101 MHz, $CDCl_3$, ppm) of **L2**.

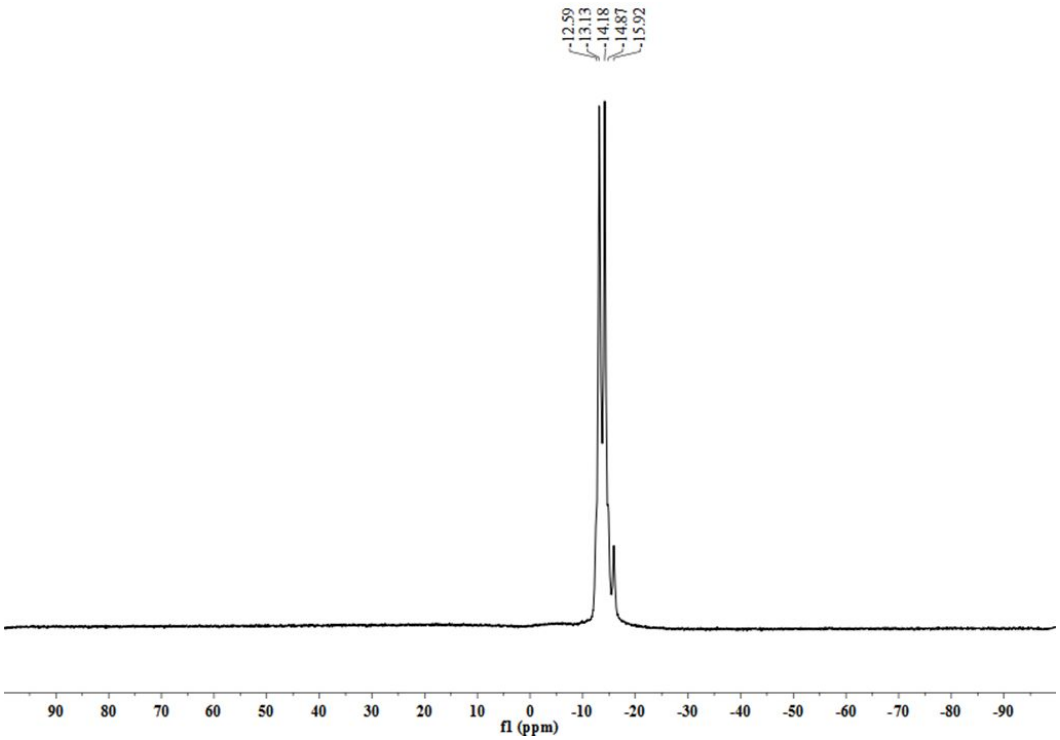

Figure S6. ^{11}B NMR (160 MHz, $CDCl_3$, ppm) of **L2**.

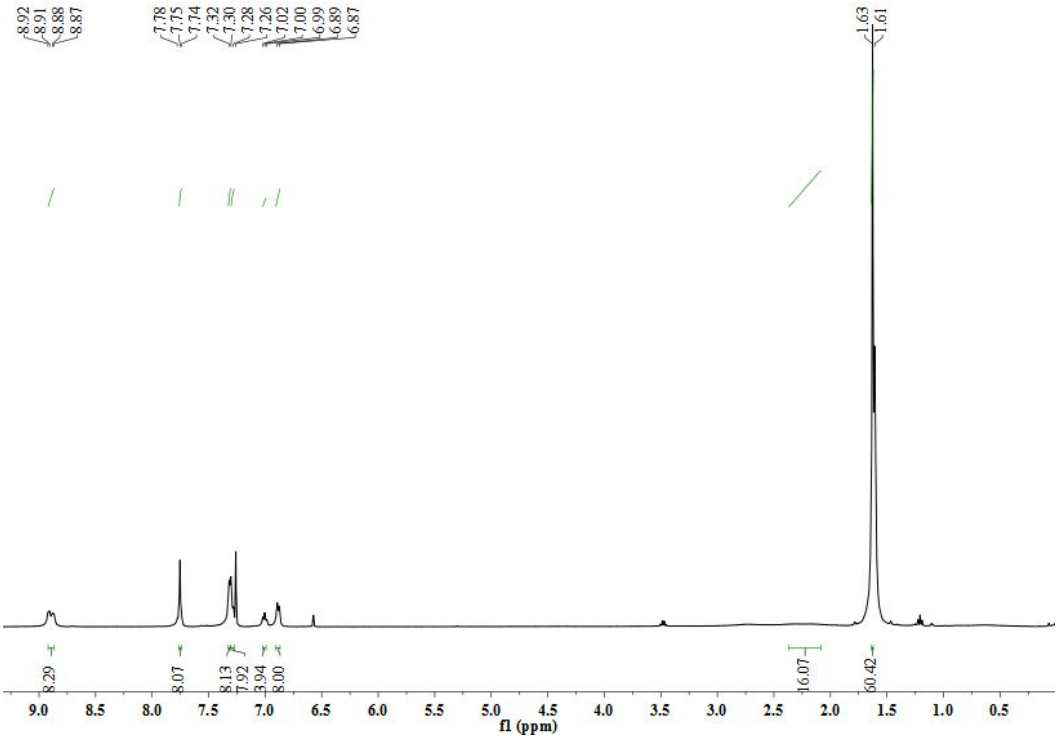

Figure S7. ^{1}H NMR (400 MHz, $CDCl_3$, ppm) of **3a**.

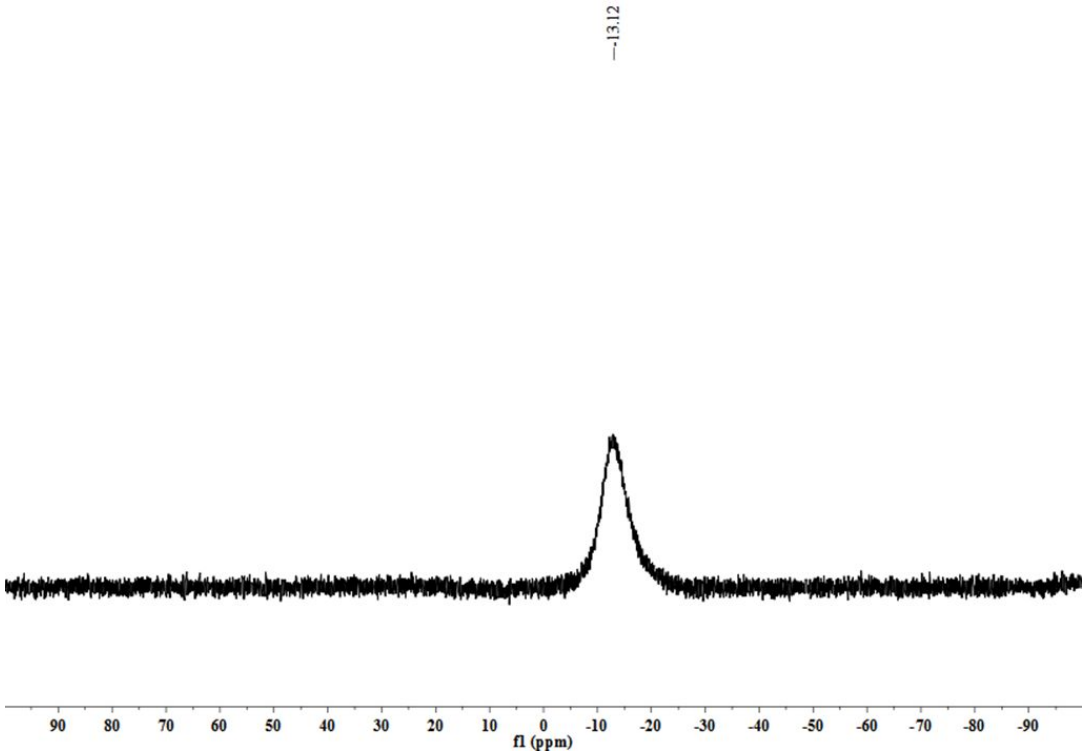

Figure S8. ^{11}B NMR (160 MHz, $CDCl_3$, ppm) of **3a**.

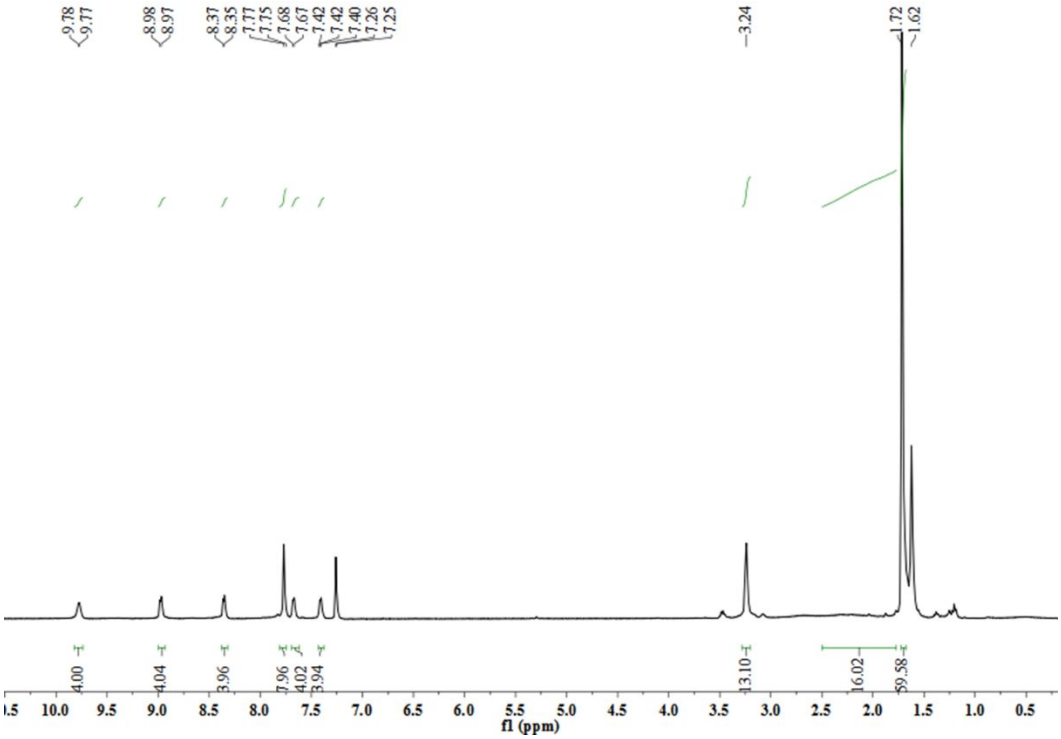

Figure S9. ^{1}H NMR (400 Hz, $CDCl_3$, ppm) of **3b**.

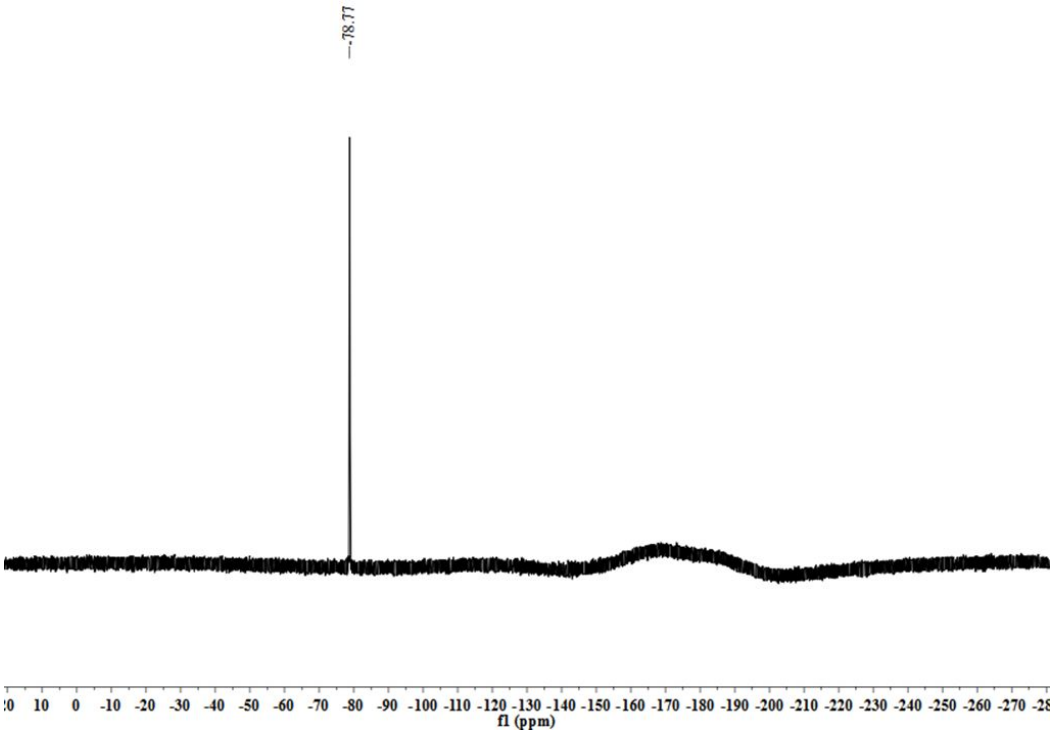

Figure S10. ^{19}F NMR (378 MHz, $CDCl_3$, ppm) of **3b**.

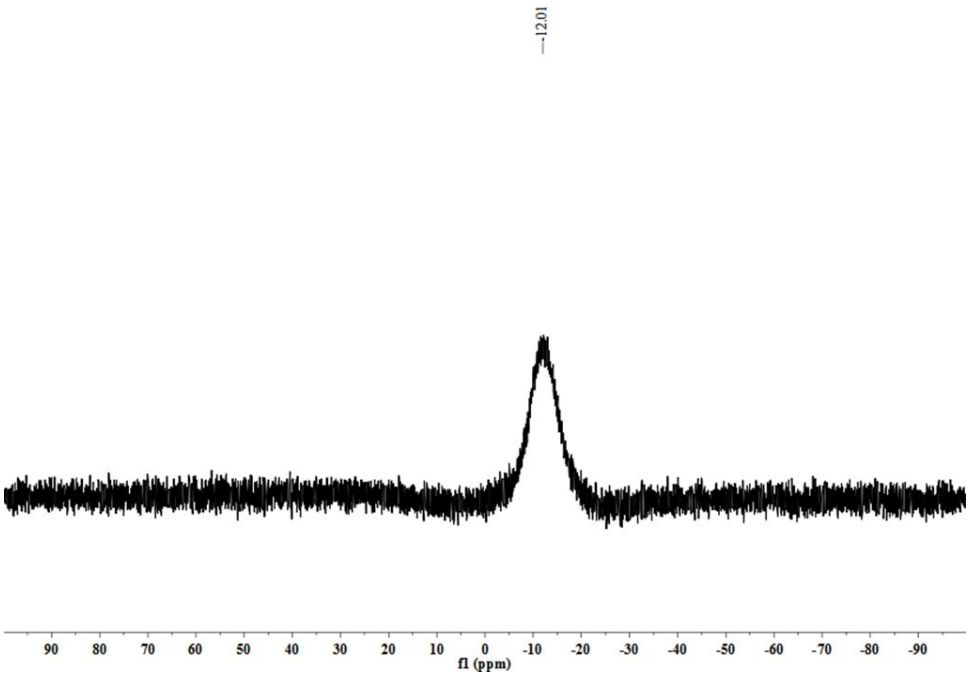

Figure S11. ^{11}B NMR (160 MHz, $CDCl_3$, ppm) of **3b**.

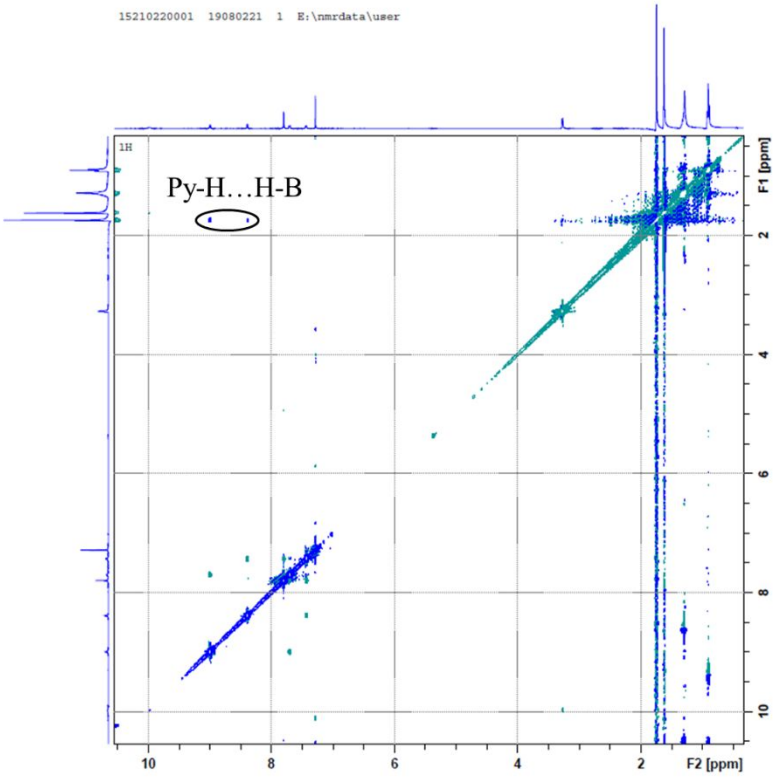

Figure S12. ^{1}H-^{1}H ROESY ($CDCl_3$, 500 MHz, 25 °C) spectrum of complex **3b** (Py: the pyridine of 1,4-di(4-pyridyl) benzene).

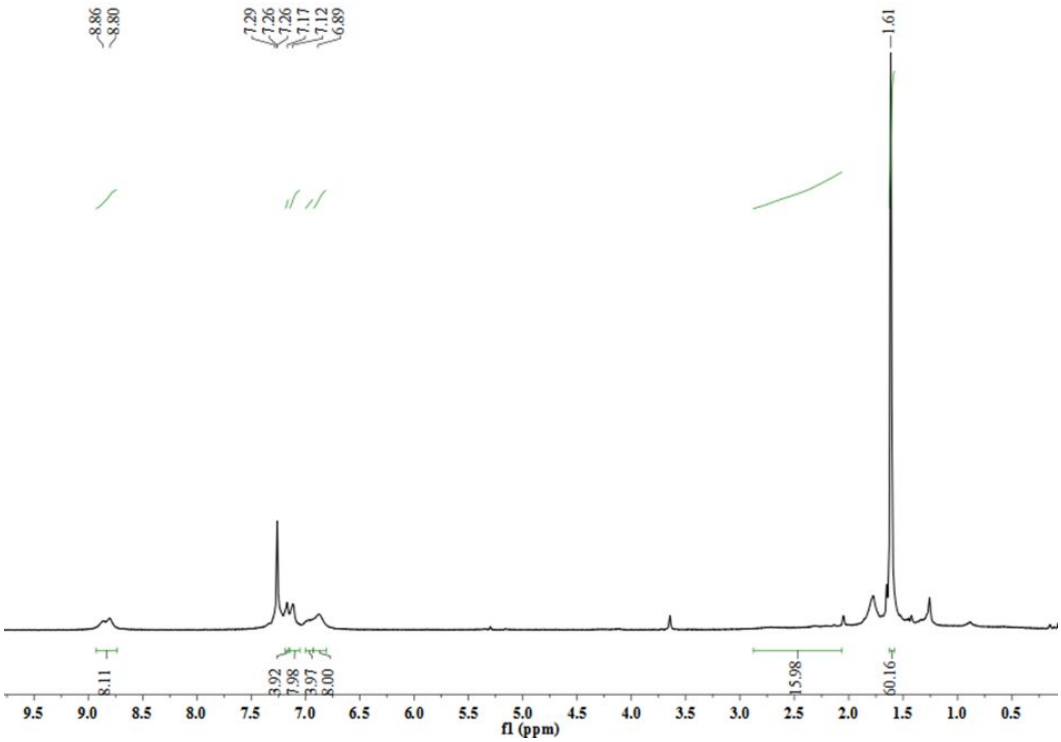

Figure S13. ^{1}H NMR (400 Hz, $CDCl_3$, ppm) spectrum of **4a**.

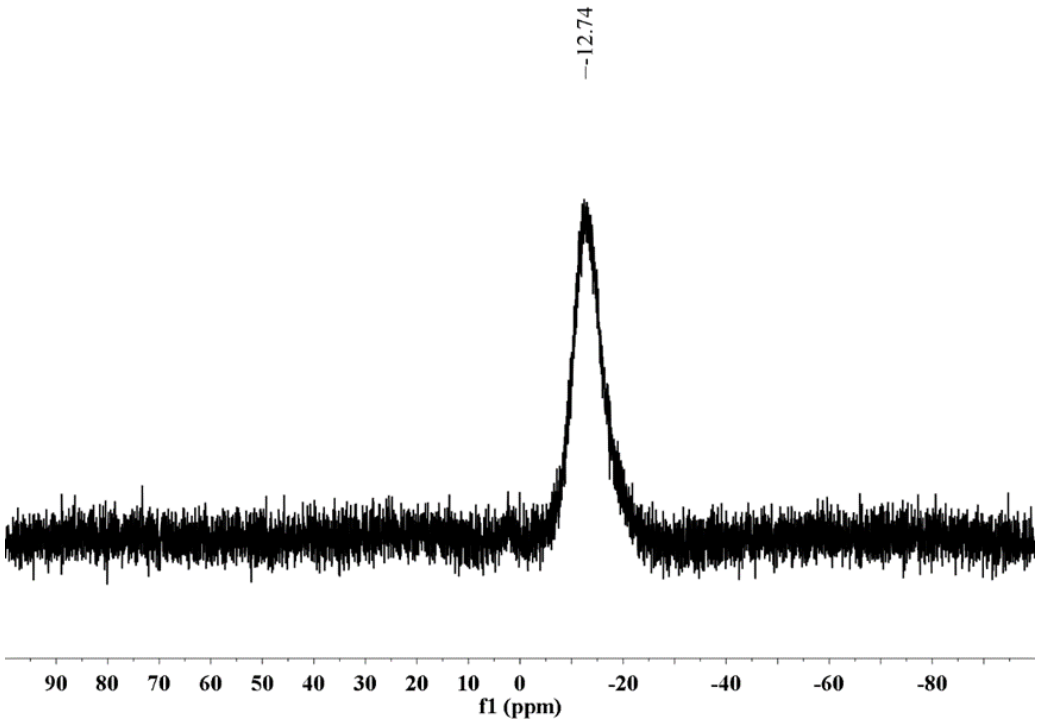

Figure S14. ^{11}B NMR (160 MHz, $CDCl_3$, ppm) of **4a**.

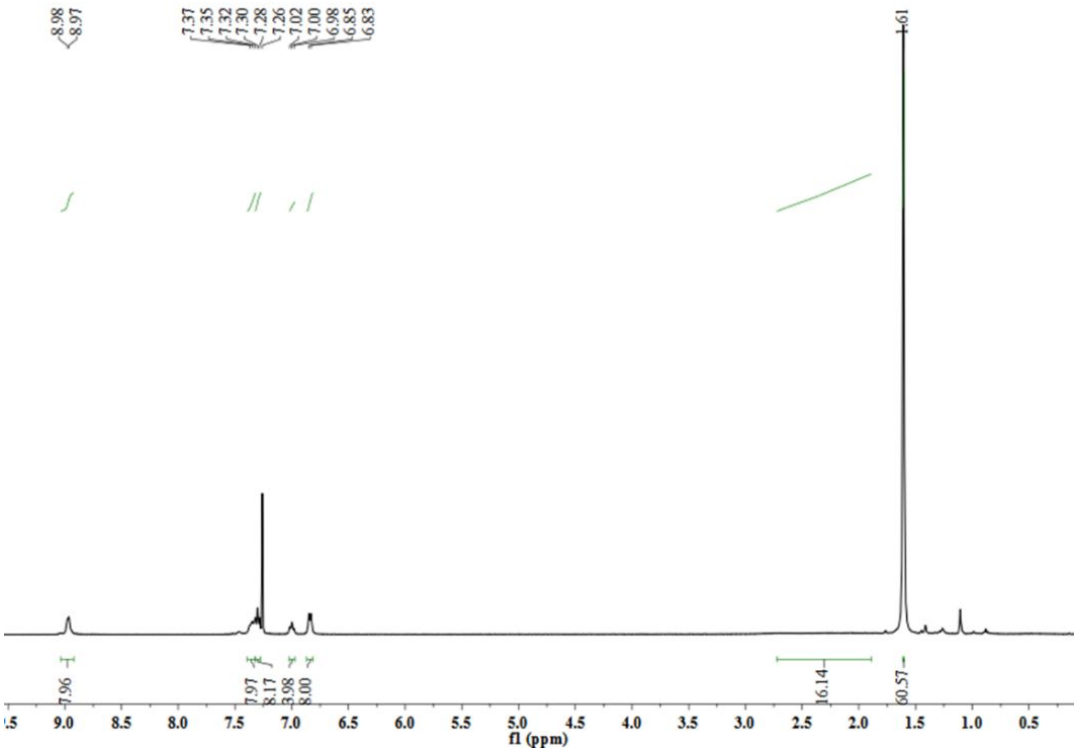

Figure S15. ^{1}H NMR (400 Hz, $CDCl_3$, ppm) spectrum of **5a**.

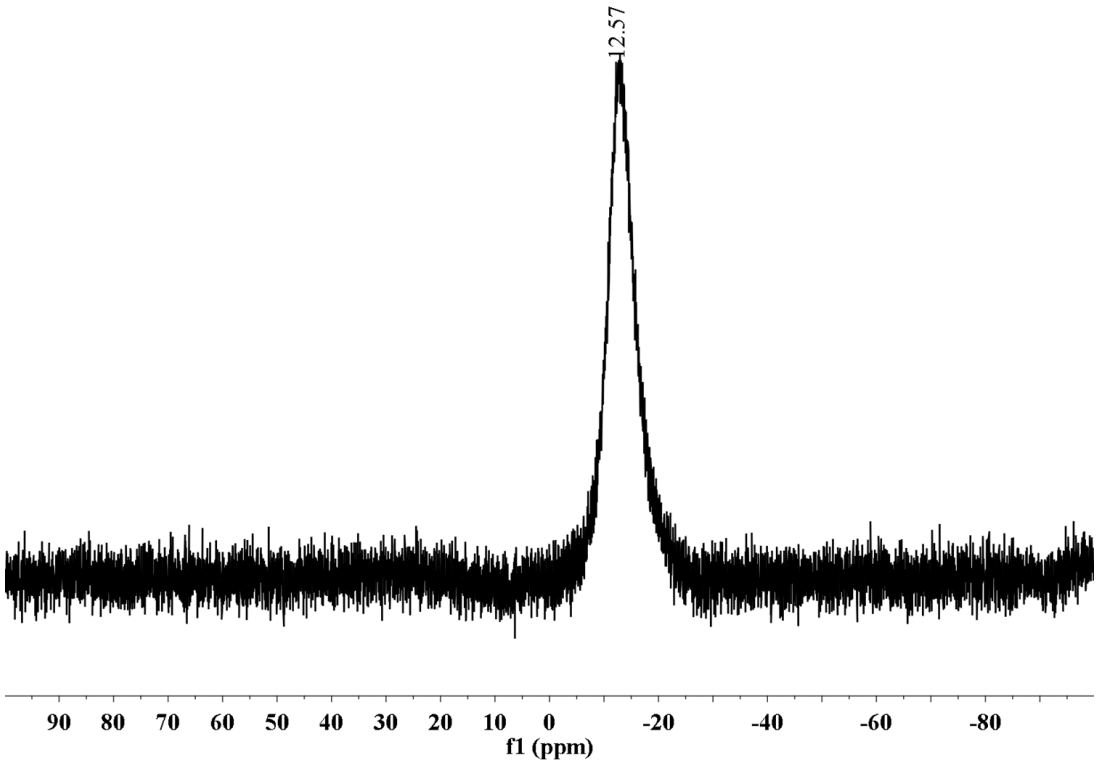

Figure S16. ^{11}B NMR (160 MHz, $CDCl_3$, ppm) of **5a**.

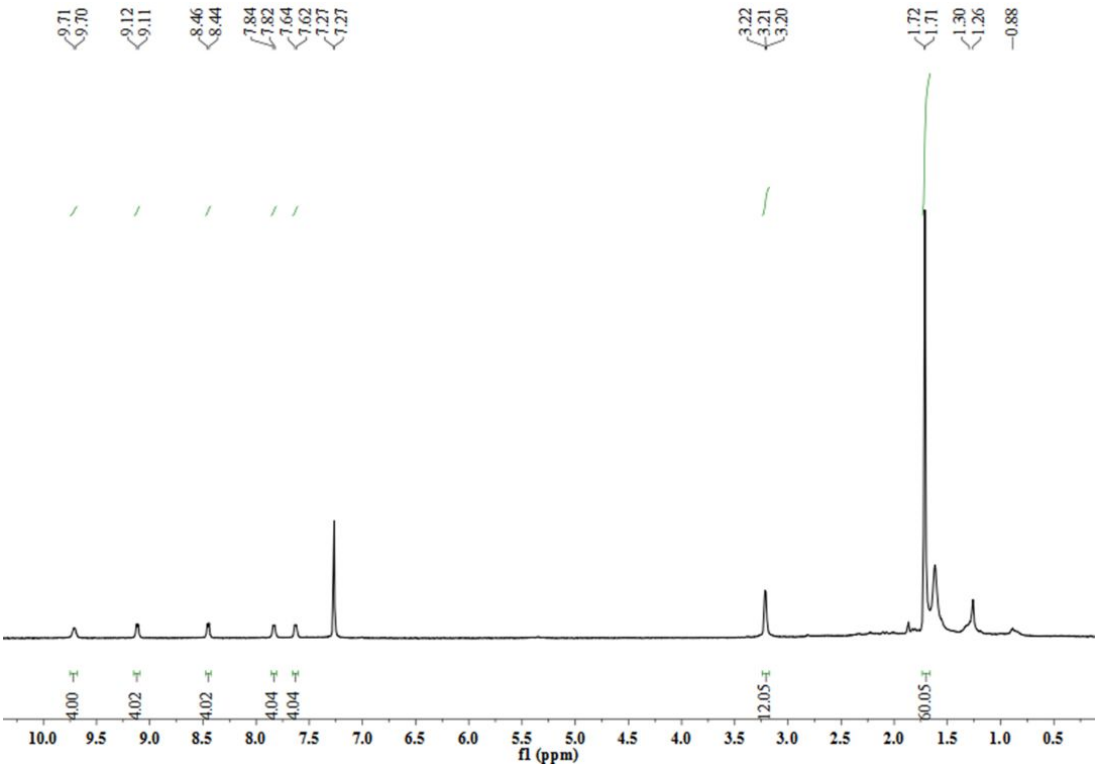

Figure S17. ^{1}H NMR (400 Hz, $CDCl_3$, ppm) spectrum of **5b**

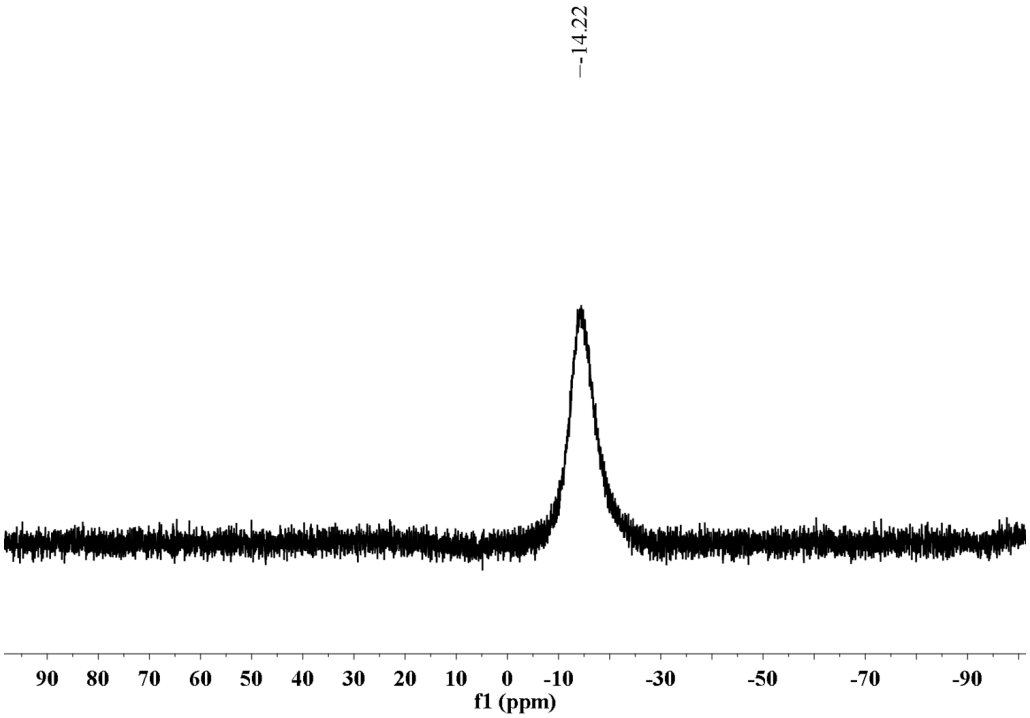

Figure S18. ^{11}B NMR (160 MHz, $CDCl_3$, ppm) of **5b**.

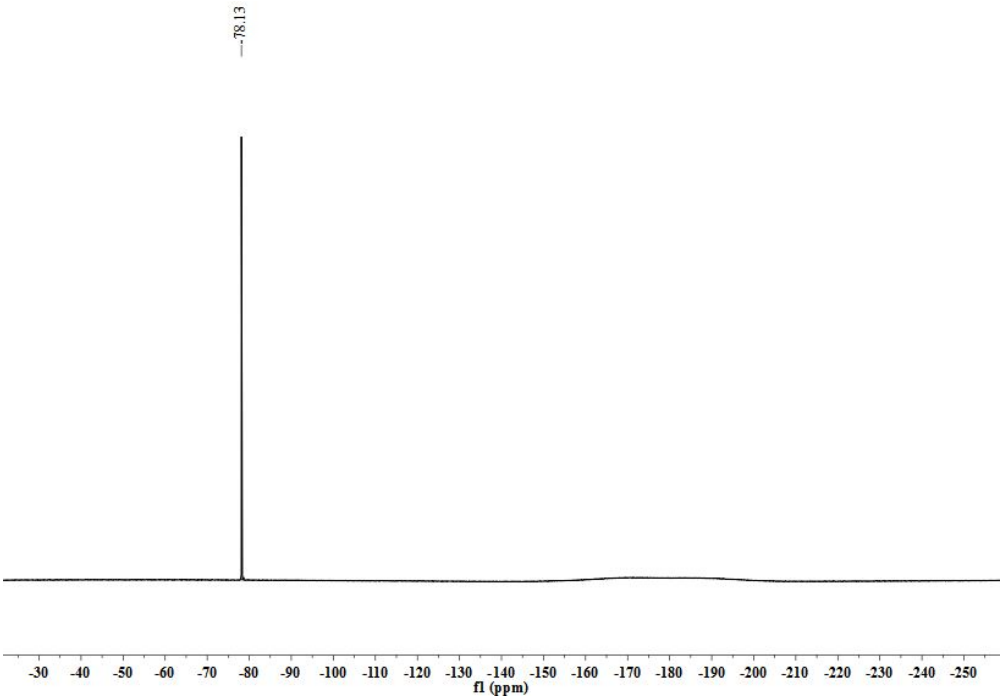

Figure S19. ^{19}F NMR (378 MHz, $CDCl_3$, ppm) of **5b**.

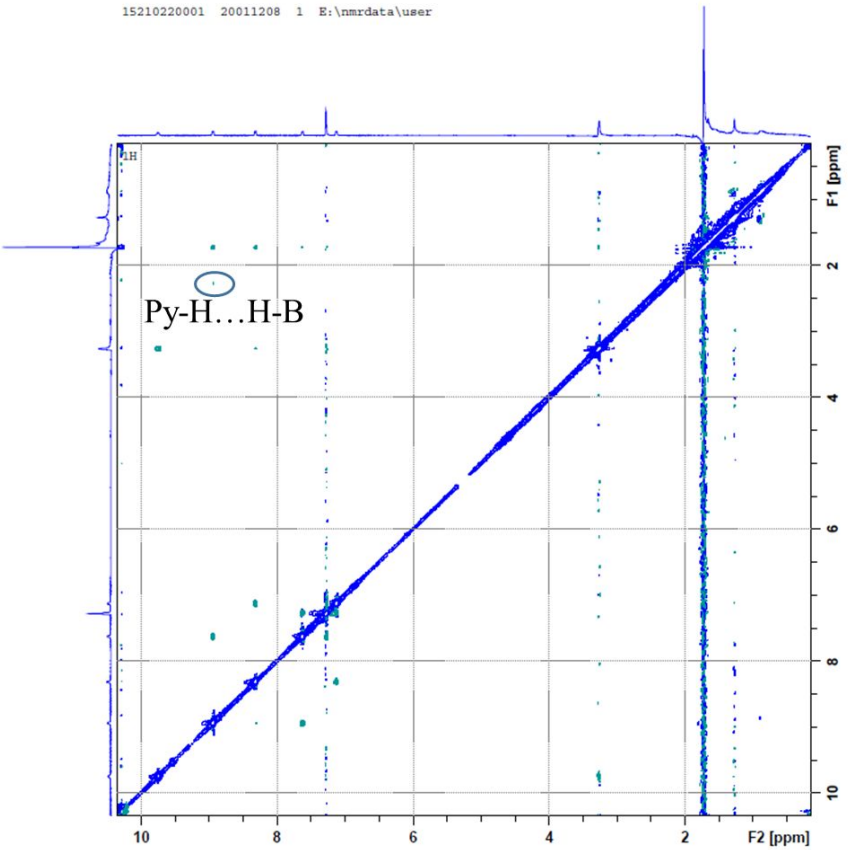

Figure S20. ^{1}H-^{1}H ROESY ($CDCl_3$, 500 MHz, 25 °C) spectrum of complex **5b** (Py: the pyridine of 1,4-di(4-pyridyl) benzene).

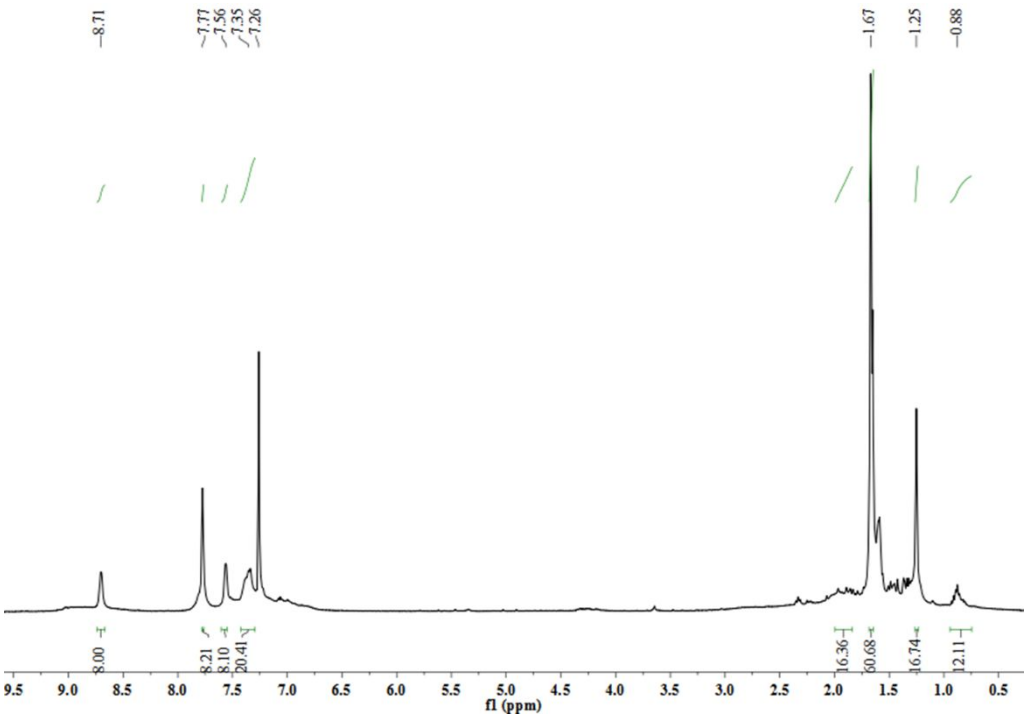

Figure S21. ^{1}H NMR (400 Hz, $CDCl_3$, ppm) of ***n*-hexane⊂3a**.

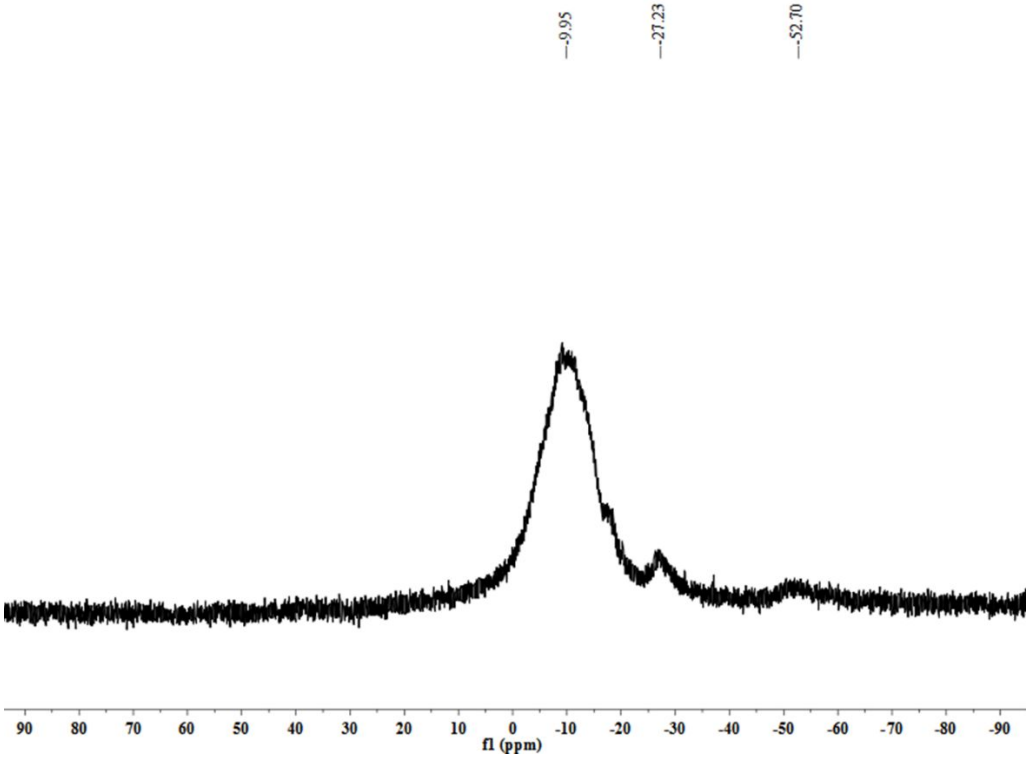

Figure S22. ^{11}B NMR (160 MHz, $CDCl_3$, ppm) of ***n*-hexane⊂3a**.

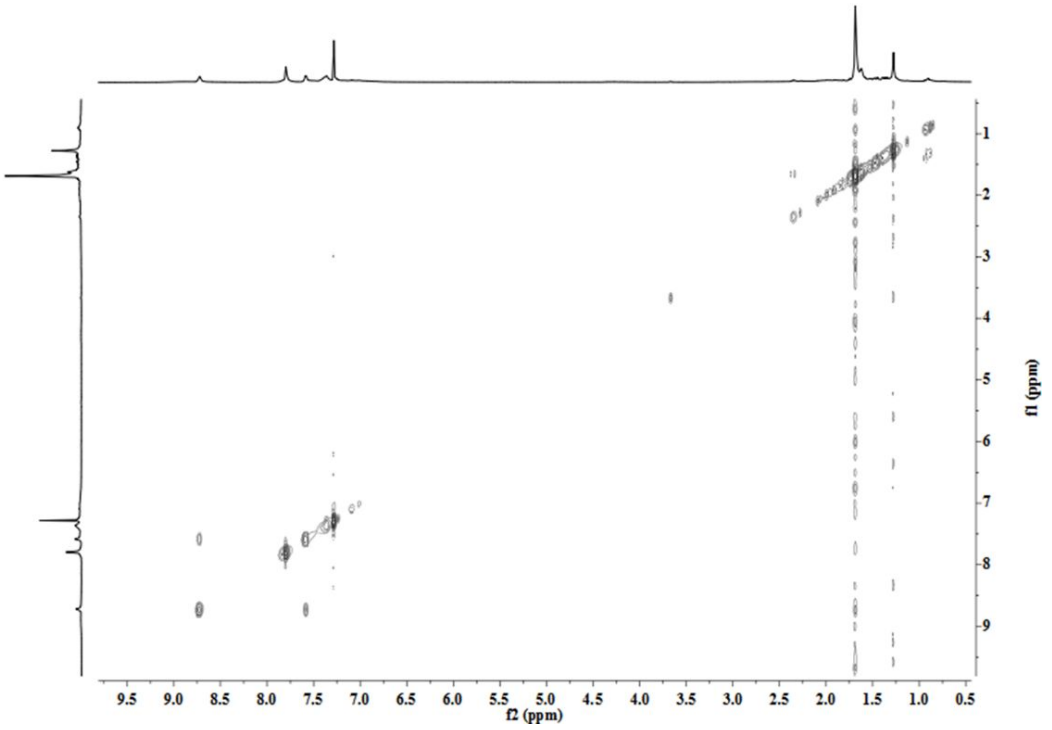

Figure S23. ^{1}H-^{1}H COSY NMR (400 MHz, $CDCl_3$, ppm) for ***n*-hexane⊂3a**.

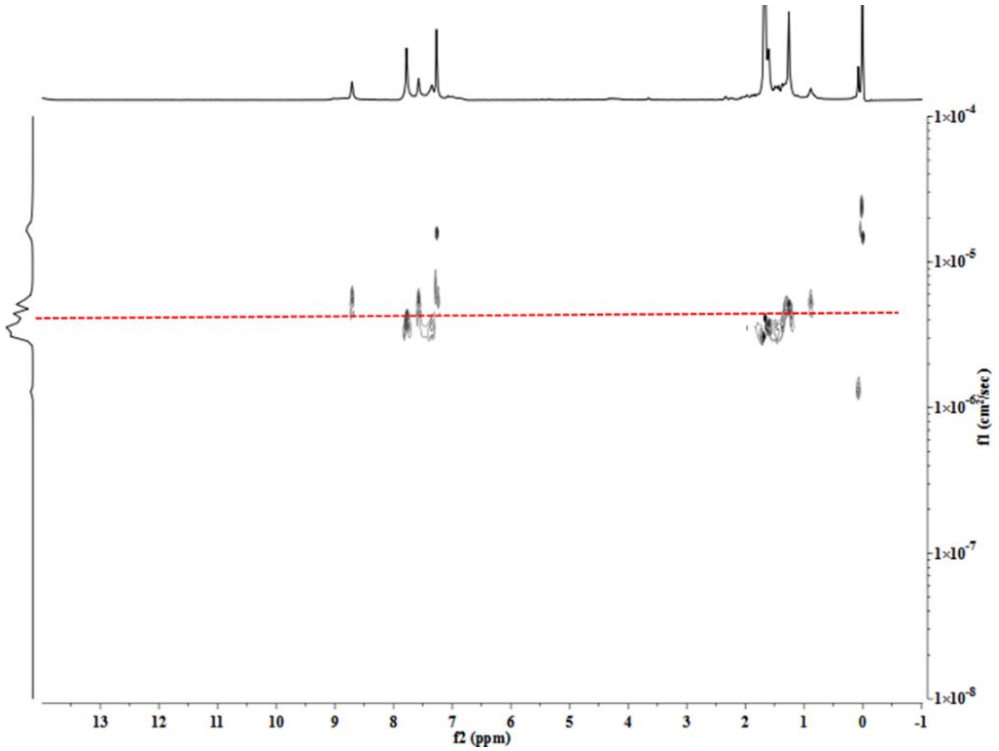

Figure S24. ^{1}H DOSY spectrum ($CDCl_3$, 400 MHz, 25 °C) of complex ***n*-hexane⊂3a**. The diffusion coefficient of 1 in $CDCl_3$ was measured to be 3.56×10^{-6} cm^2 s^{-1}.

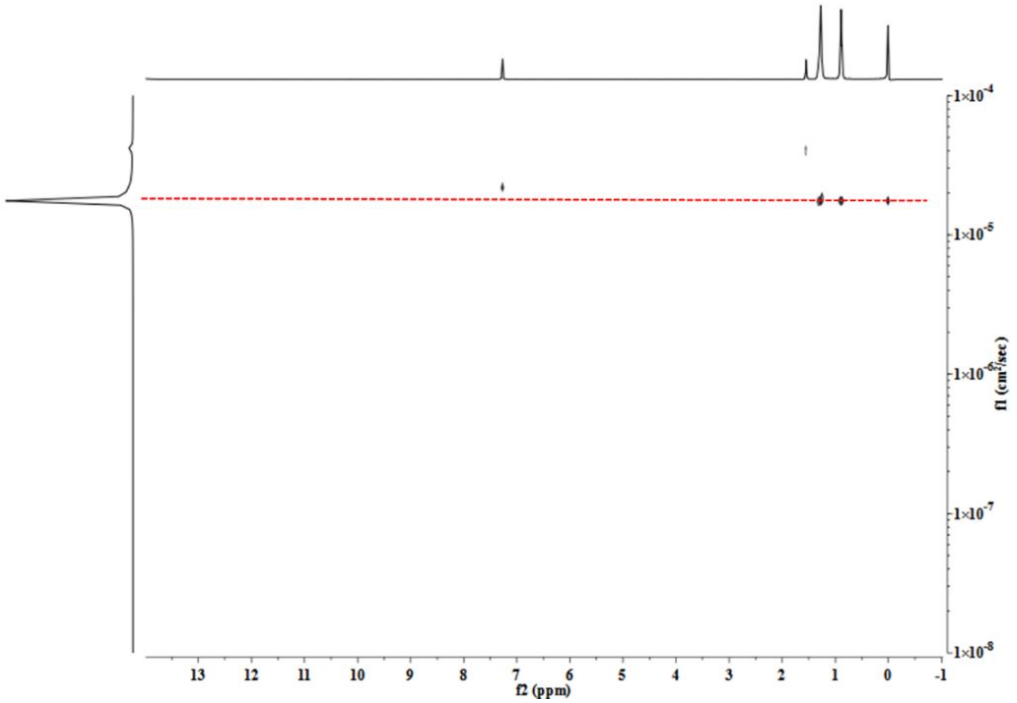

Figure S25. ^{1}H DOSY spectrum ($CDCl_3$, 400 MHz, 25 °C) of free *n*-hexane. The diffusion coefficient of 1 in $CDCl_3$ was measured to be 4.75×10^{-5} cm^2 s^{-1}.

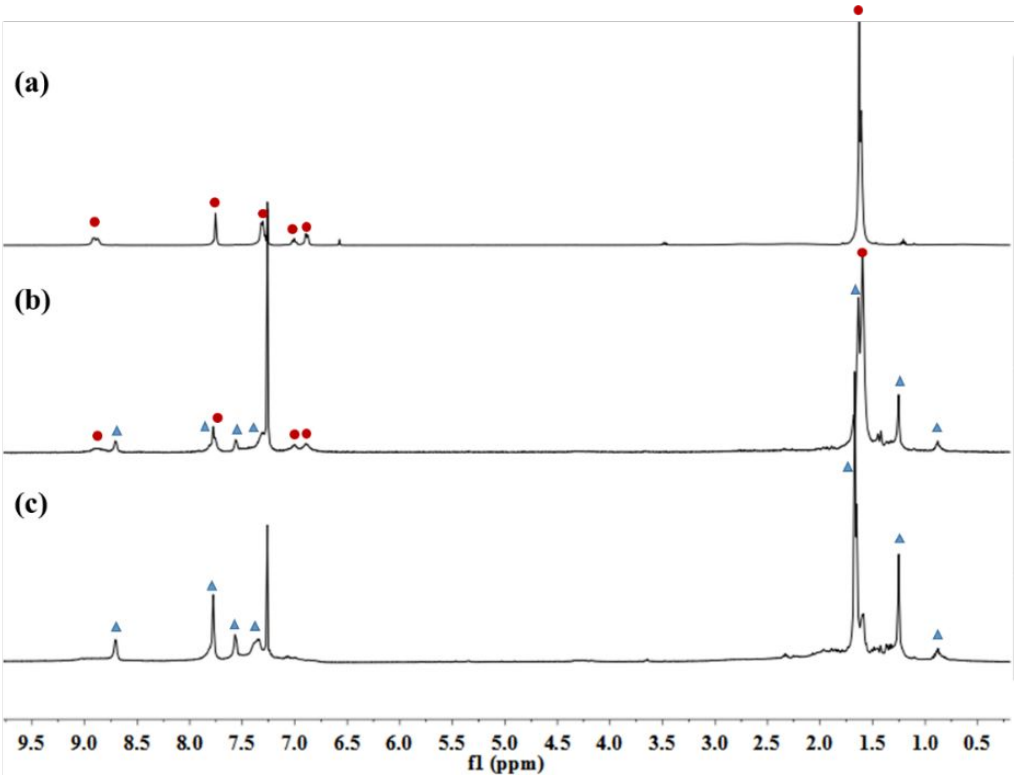

Figure S26. ^{1}H NMR (298K, 400 MHz, $CDCl_3$, ppm) for transformation from **3a** to ***n*-hexane⊂3a**. (a) complex **3a**, (b) *n*-hexane: complex **3a** = 1: 1, (c) complex ***n*-hexane⊂3a**. Green triangles denote complex **3a** signals; red circles denote complex ***n*-hexane⊂3a** signals.

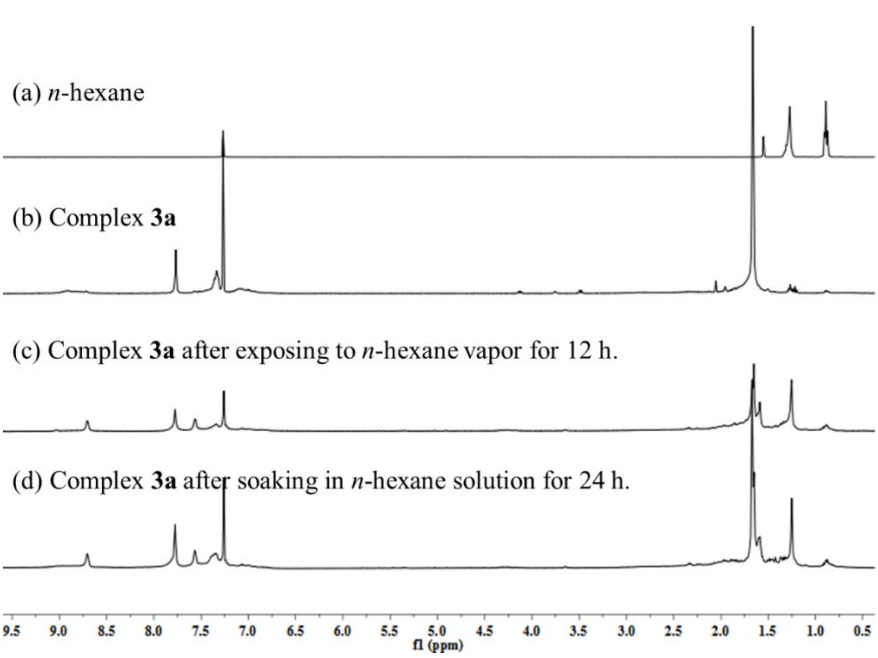

Figure S27. ^{1}H NMR spectrum (298K, 400 MHz, $CDCl_3$, ppm) (a) *n*-hexane; (b) complex **3a** after heating at 60 °C under vacuo; (c) complex **3a** after exposing to *n*-hexane vapor for 12 h; (d) complex **3a** after soaking in *n*-hexane solution for 24h. The proton signals change in the spectrum. It indicates that the complex **3a** can uptake *n*-hexane both in vapour and solution system.

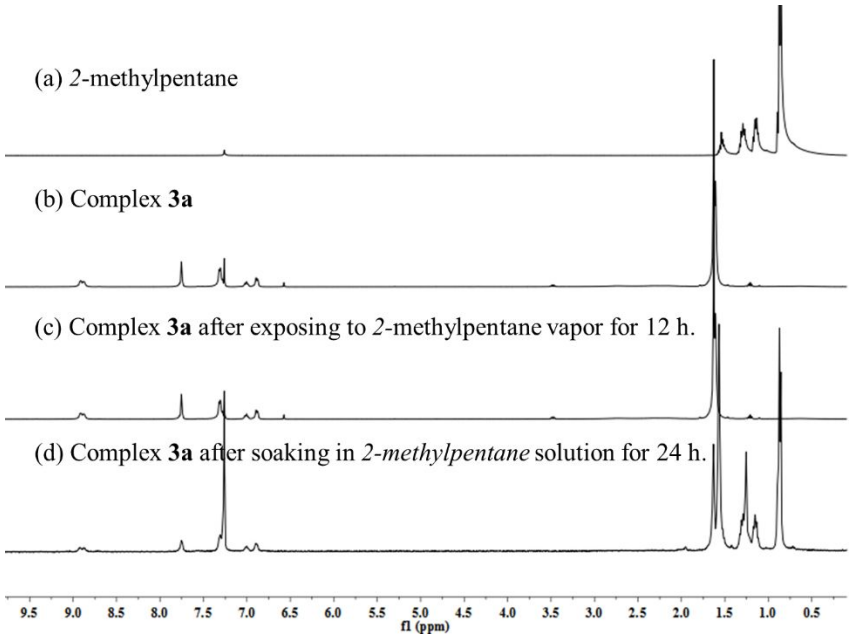

Figure S28. ^{1}H NMR spectrum (298K, 400 MHz, $CDCl_3$, ppm) (a) *2*-methylpentane; (b) complex **3a** after heating at 60 °C under vacuo; (c) complex **3a** after exposing to *2*-methylpentane vapor for 12 h; (d) complex **3a** after soaking in *2*-methylpentane solution for 24h. The proton signals don't change in the spectrum. It indicates that the complex **3a** can't uptake *2*-methylpentane both in vapour and solution system.

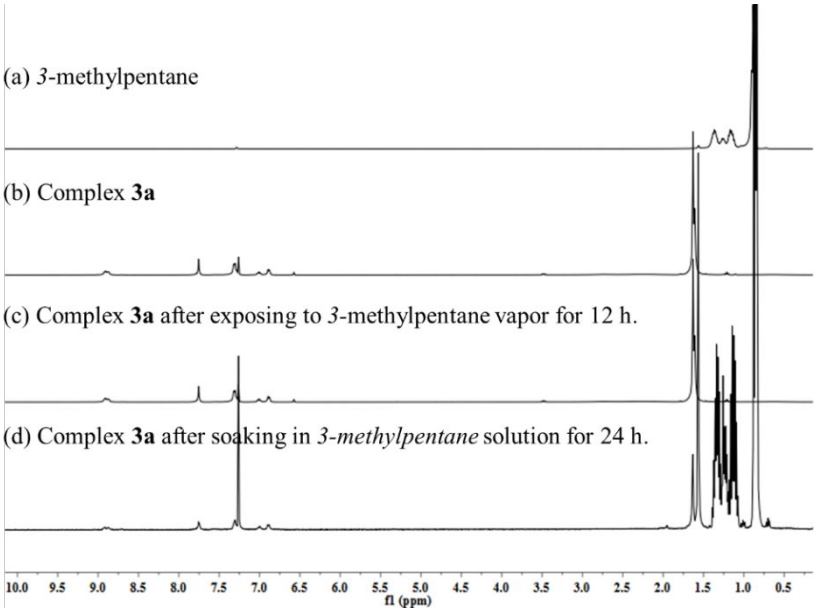

Figure S29. ^{1}H NMR spectrum (298K, 400 MHz, $CDCl_3$, ppm) (a) *3*-methylpentane; (b) complex **3a** after heating at 60 °C under vacuo; (c) complex **3a** after exposing to *3*-methylpentane vapor for 12 h; (d) complex **3a** after soaking in *3*-methylpentane solution for 24h. The proton signals don't change in the spectrum. It indicates that the complex **3a** can't uptake *2*-methylpentane both in vapour and solution system.

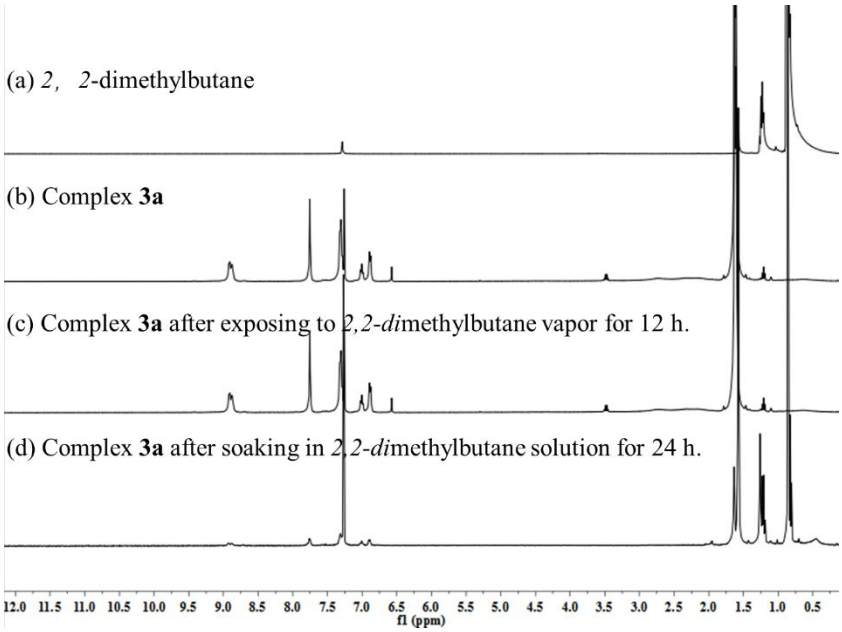

Figure S30. ^{1}H NMR spectrum (298K, 400 MHz, $CDCl_3$, ppm) (a) *2,2*-dimethylbutane; (b) complex **4a** after heating at 60 °C under vacuo; (c) complex **4a** after exposing to *2,2*-dimethylbutane vapor for 12 h; (d) complex **4a** after soaking in *2,2*-dimethylbutane solution for 24h. The proton signals don't change in the spectrum. It indicates that the complex **4a** can't uptake *2,2*-dimethylbutane both in vapour and solution system.

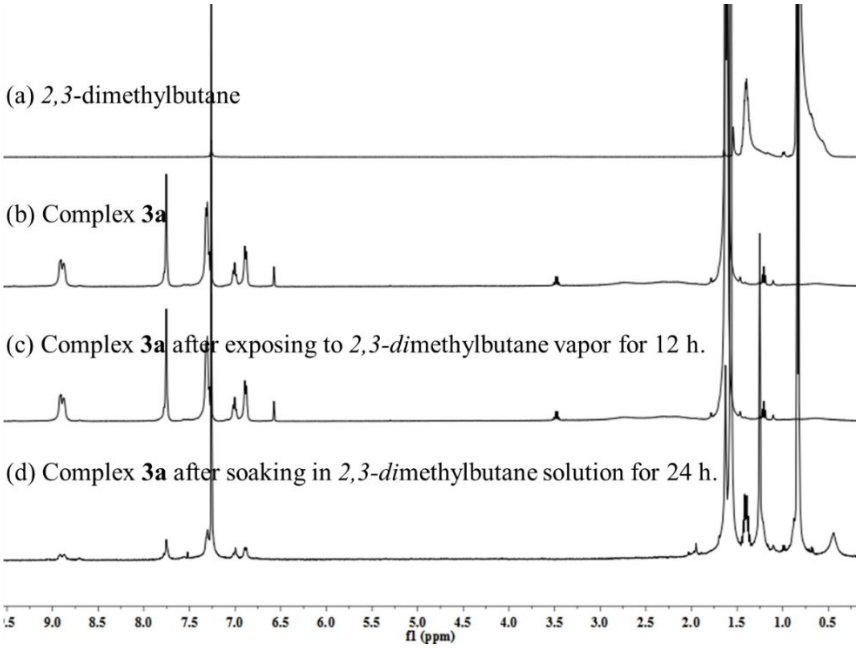

Figure S31. ^{1}H NMR spectrum (298K, 400 MHz, $CDCl_3$, ppm) (a) *2,3*-dimethylbutane; (b) complex **4a** after heating at 60 °C under vacuo; (c) complex **4a** after exposing to *2,3*-dimethylbutane vapor for 12 h; (d) complex **4a** after soaking in *2,3*-dimethylbutane solution for 24h. The proton signals don't change in the spectrum. It indicates that the complex **4a** can't uptake *2,3*-dimethylbutane both in vapour and solution system.

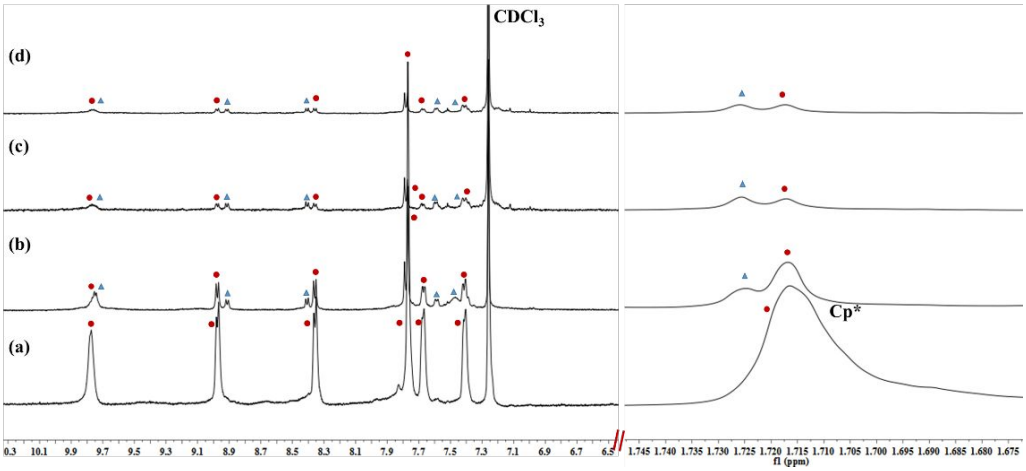

Figure S32. Partial ^{1}H NMR (298K, 400 MHz, $CDCl_3$, ppm) for transformation from **3b** to ***n*-hexane⊂3b**. (a) complex **3b**, (b) *n*-hexane: complex **3b** = 2: 1, (c) *n*-hexane: complex **3b** = 2: 1 one day later: (d) *n*-hexane: complex **3b** = 2: 1 three days later. Green triangles denote complex ***n*-hexane⊂3b** signals; red circles denote complex **3b** signals. The solubility of complex ***n*-hexane⊂3b** is very poor, so in the end the signals are very weak.

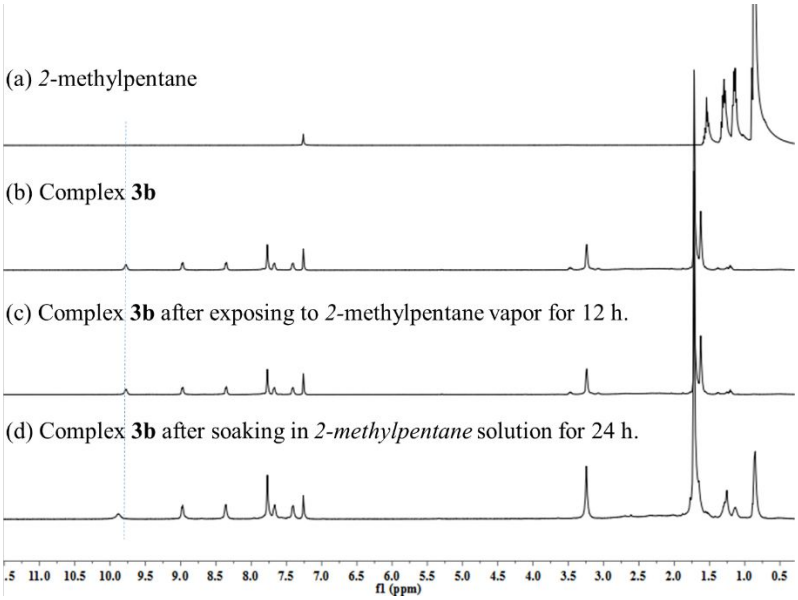

Figure S33. ^{1}H NMR spectrum (298K, 400 MHz, $CDCl_3$, ppm) (a) *2*-methylpentane; (b) complex **4b** after heating at 60 °C under vacuo; (c) complex **3b** after exposing to *2*-methylpentane vapor for 12 h; (d) complex **3b** after soaking in *2*-methylpentane solution for 24h. The proton signals don't change in the spectrum except for N-H protons. It indicates that the complex **3b** can't uptake *2*-methylpentane both in vapour and solution system.

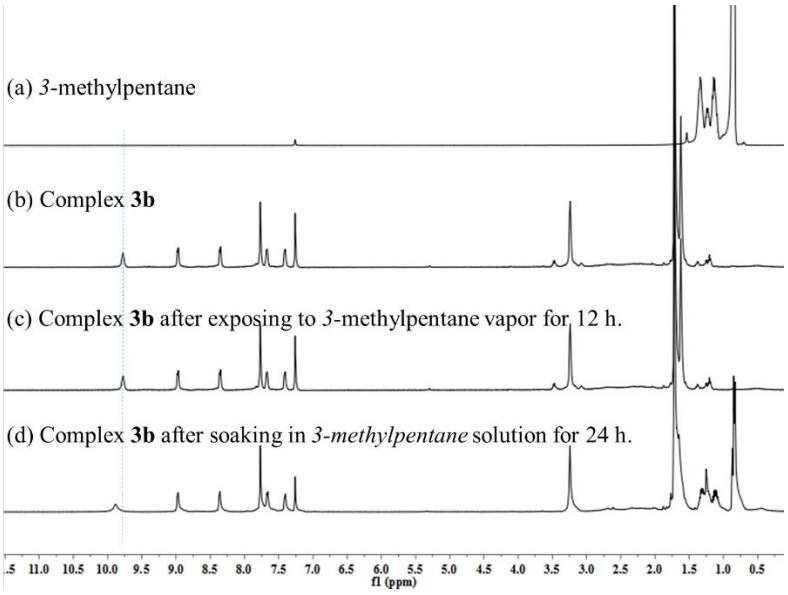

Figure S34. ^{1}H NMR spectrum (298K, 400 MHz, $CDCl_3$, ppm) (a) *3*-methylpentane; (b) complex **3b** after heating at 60 °C under vacuo; (c) complex **3b** after exposing to *3*-methylpentane vapor for 12 h; (d) complex **3b** after soaking in *3*-methylpentane solution for 24h. The proton signals don't change in the spectrum except for N-H protons. It indicates that the complex **3b** can't uptake *2*-methylpentane both in vapour and solution system.

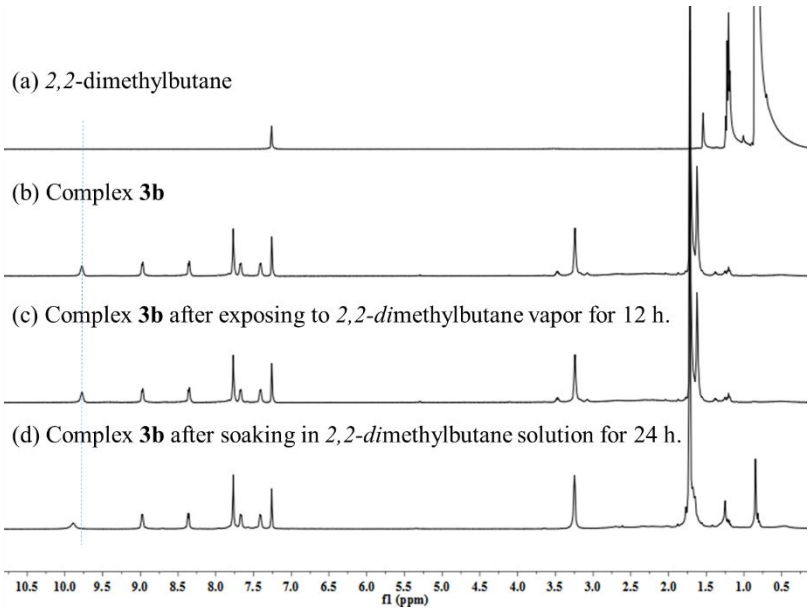

Figure S35. ^{1}H NMR spectrum (298K, 400 MHz, $CDCl_3$, ppm) (a) *2,2*-dimethylbutane; (b) complex **3b** after heating at 60 °C under vacuo; (c) complex **3b** after exposing to *2,2*-dimethylbutane vapor for 12 h; (d) complex **3b** after soaking in *2,2*-dimethylbutane solution for 24h. The proton signals don't change except for N-H protons in the spectrum. It indicates that the complex **3b** can't uptake *2,2*-dimethylbutane both in vapour and solution system.

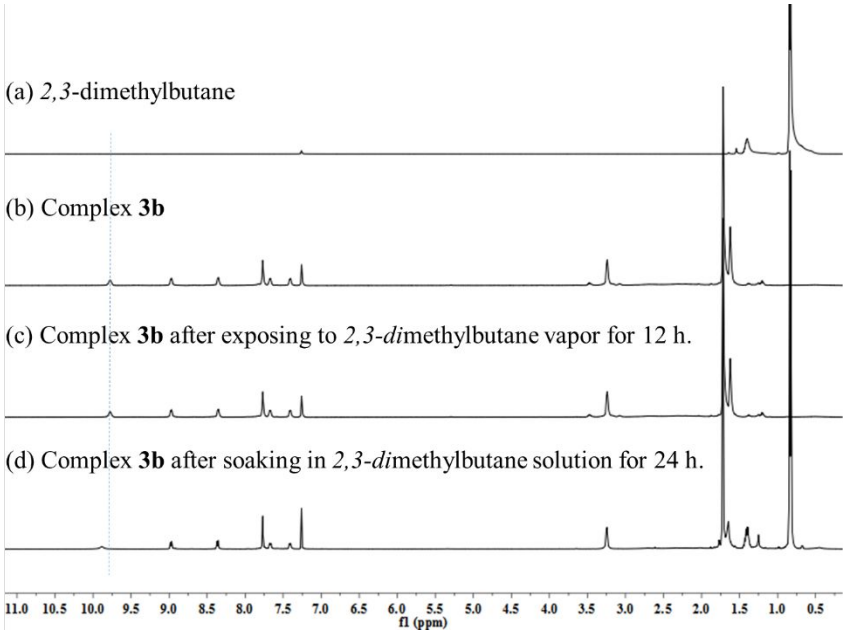

Figure S36. ^{1}H NMR spectrum (298K, 400 MHz, $CDCl_3$, ppm) (a) *2,3*-dimethylbutane; (b) complex **3b** after heating at 60 °C under vacuo; (c) complex **3b** after exposing to *2,3*-dimethylbutane vapor for 12 h; (d) complex **3b** after soaking in *2,2*-dimethylbutane solution for 24h. The proton signals don't change except for N-H protons in the spectrum. It indicates that the complex **3b** can't uptake *2,3*-dimethylbutane both in vapour and solution system.

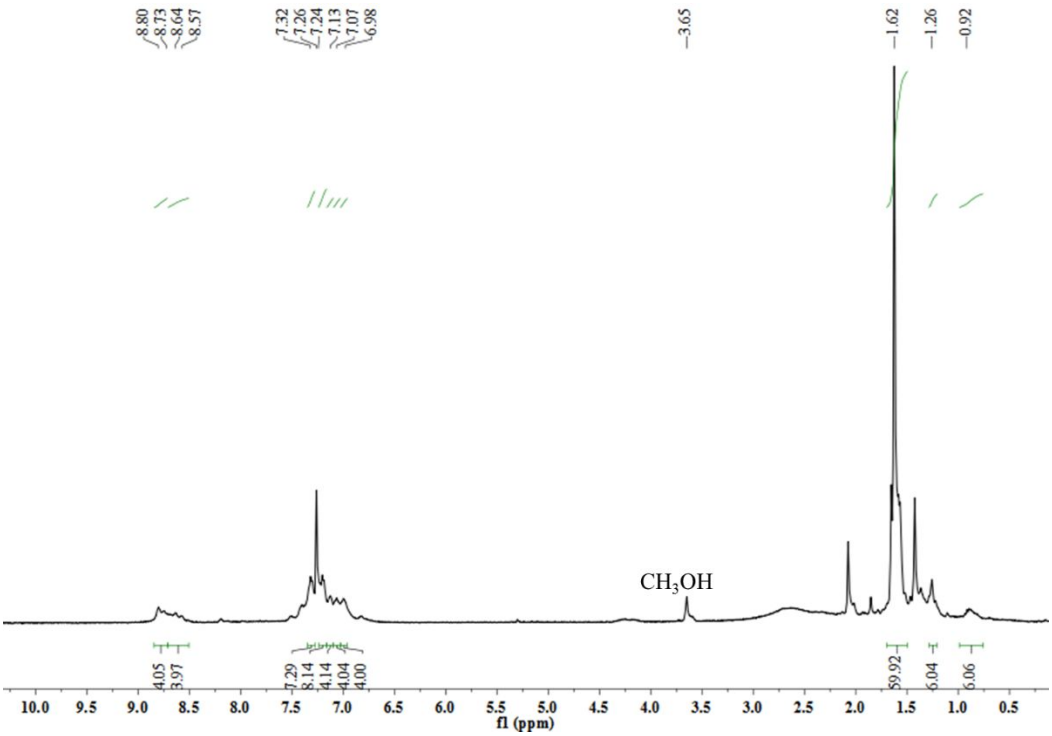

Figure S37. ^{1}H NMR (400 Hz, $CDCl_3$, ppm) of ***n*-pentane⊂4a**.

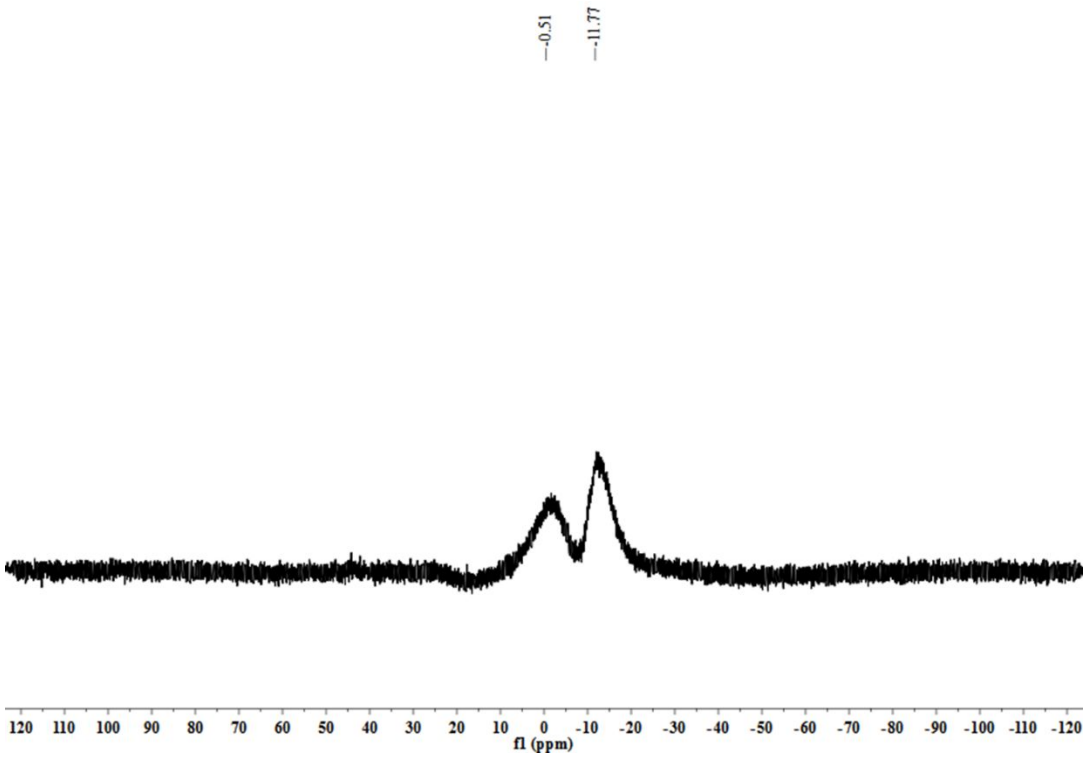

Figure S38. ^{11}B NMR (160 MHz, $CDCl_3$, ppm) of ***n*-pentane⊂4a**.

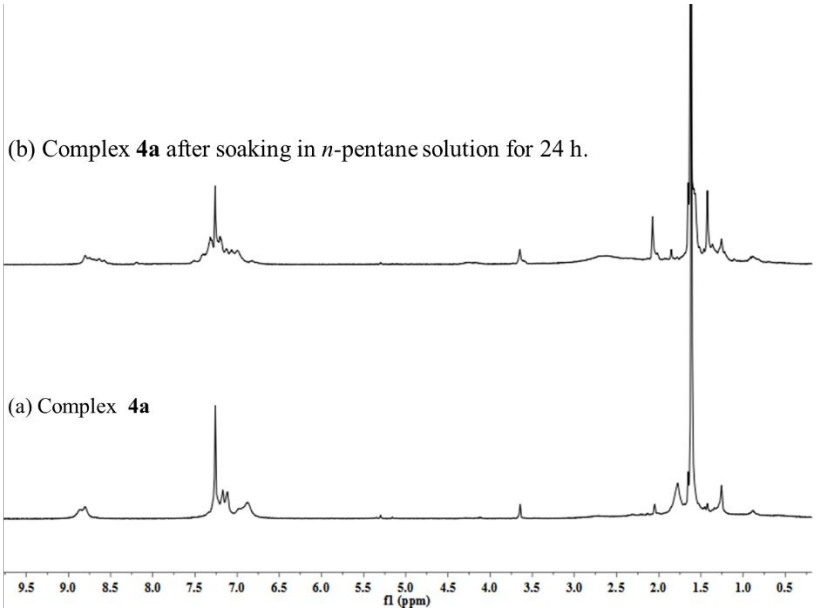

Figure S39. ^{1}H NMR spectrum (298K, 400 MHz, $CDCl_3$, ppm) (a) Complex **4a**; (b) Complex **4a** after soaking in *n*-pentane solution for 24h. The changing proton signals indicates the interaction between *n*-pentane and complex **4a**.

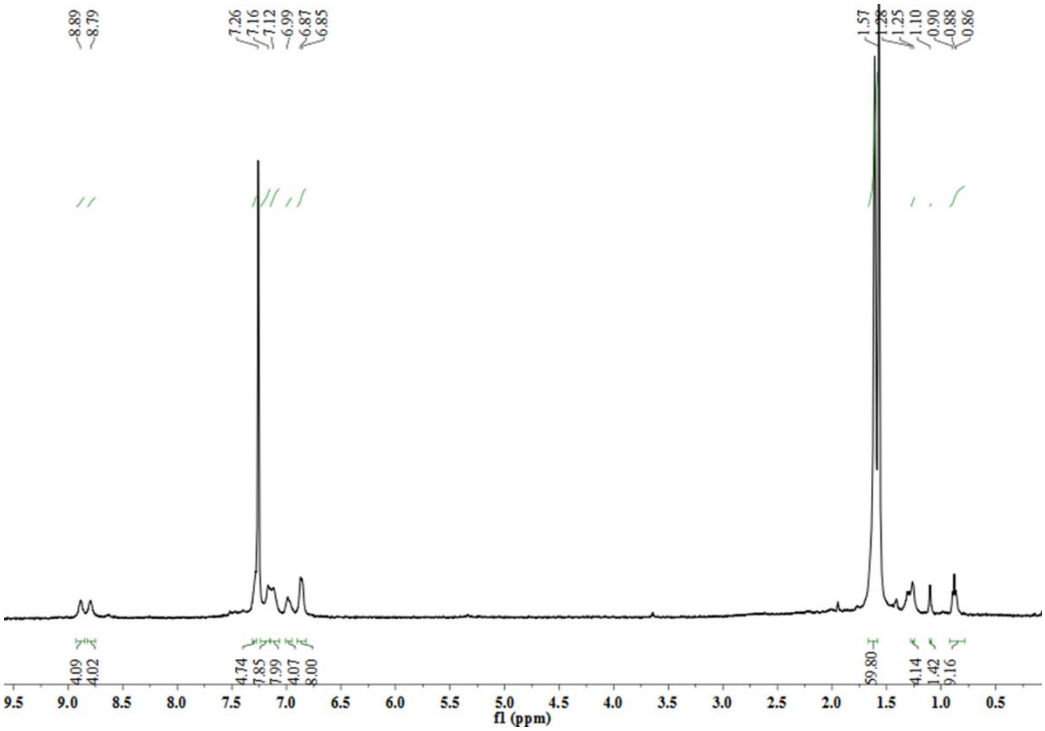

Figure S40. ^{1}H NMR (400 Hz, $CDCl_3$, ppm) of ***2*-methylpentane⊂4a**.

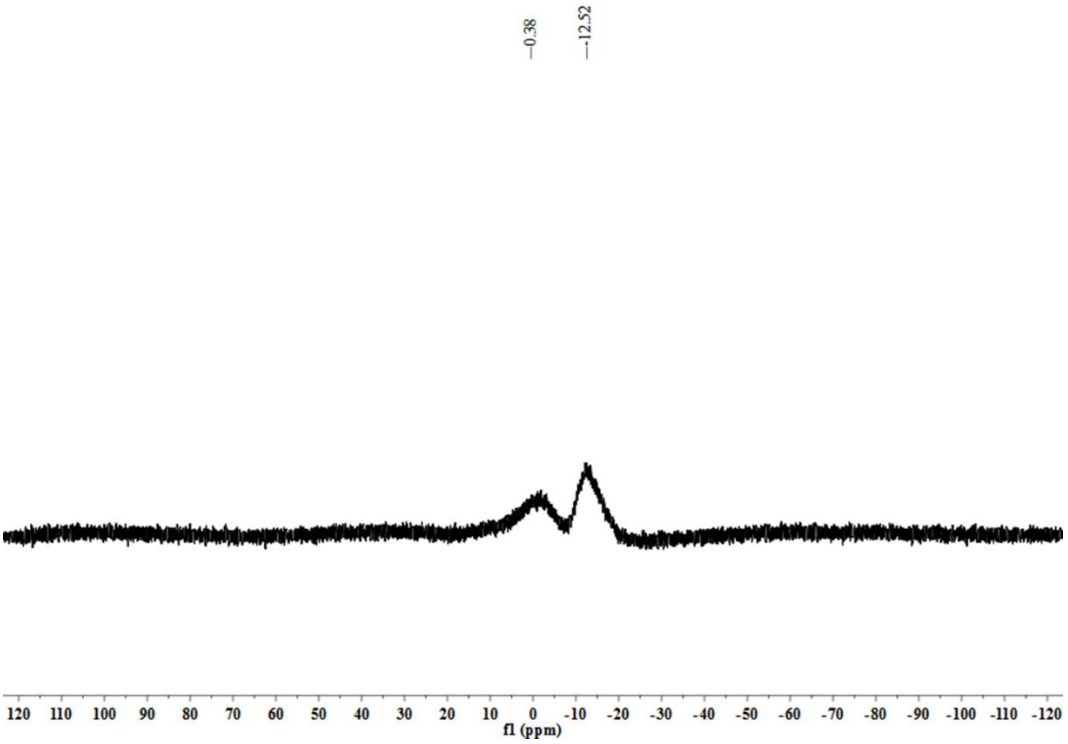

Figure S41. ^{11}B NMR (160 MHz, $CDCl_3$, ppm) of ***2*-methylpentane⊂4a**.

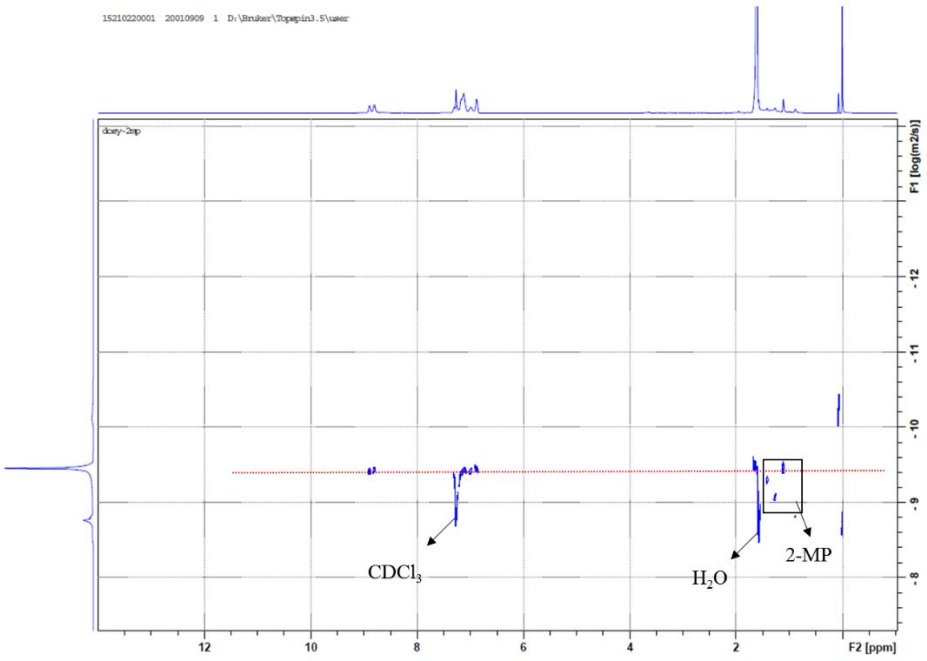

Figure S42. ^{1}H DOSY spectrum ($CDCl_3$, 400 MHz, 25 °C) of complex ***2*-methylpentane⊂4a**.

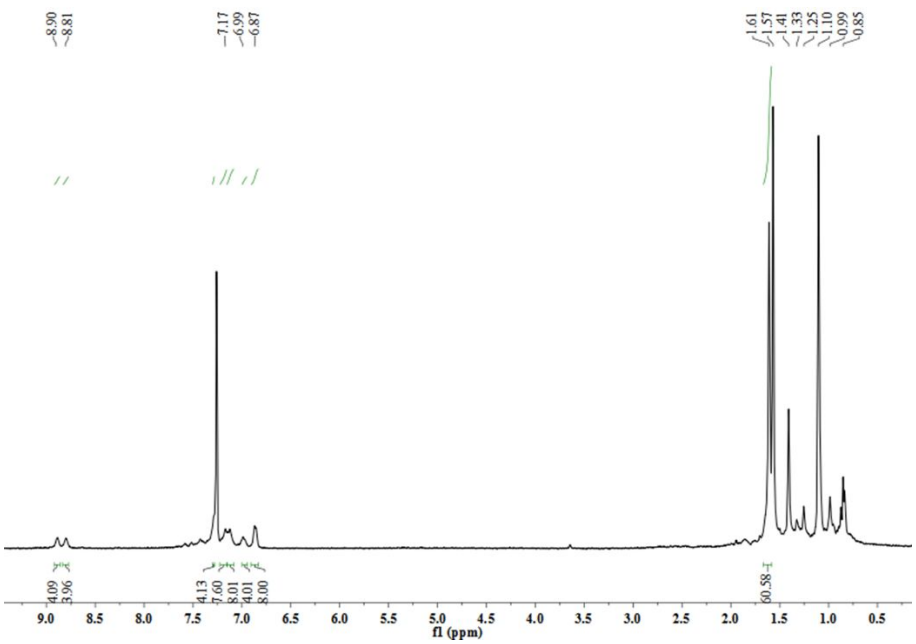

Figure S43. ^{1}H NMR (400 Hz, $CDCl_3$, ppm) of ***3*-methylpentane⊂4a**.

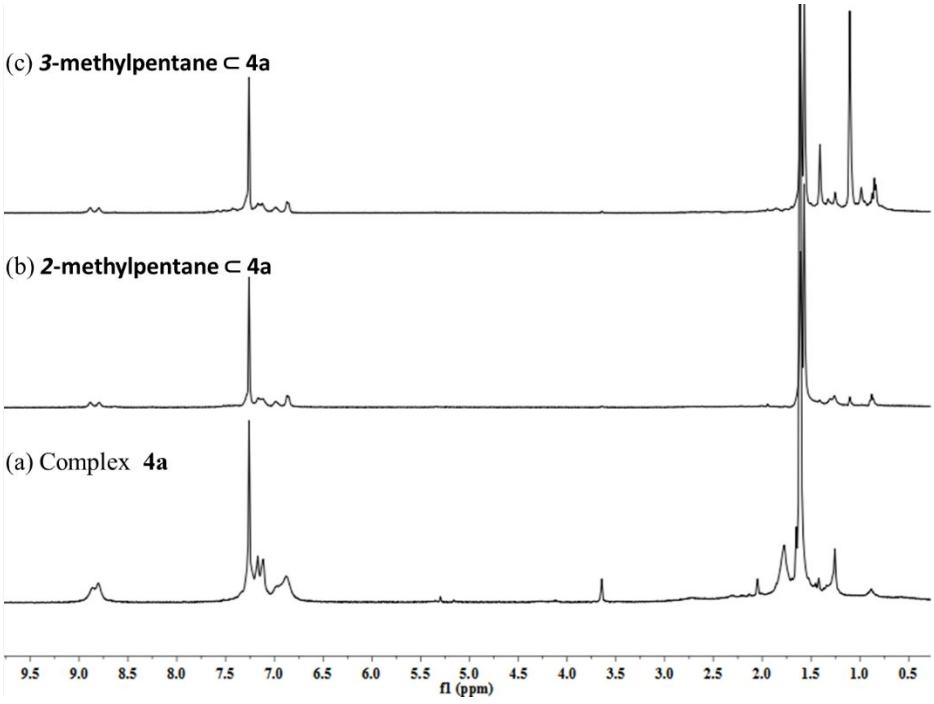

Figure S44. ^{1}H NMR spectrum (298K, 400 MHz, $CDCl_3$, ppm) (a) Complex **4a**; (b) Complex ***2*-methylpentane⊂4a**; (c) Complex ***3*-methylpentane⊂4a**. The changing proton signals indicates the interaction between *2*-methylpetane/ *3*-methylpentane and complex **4a**.

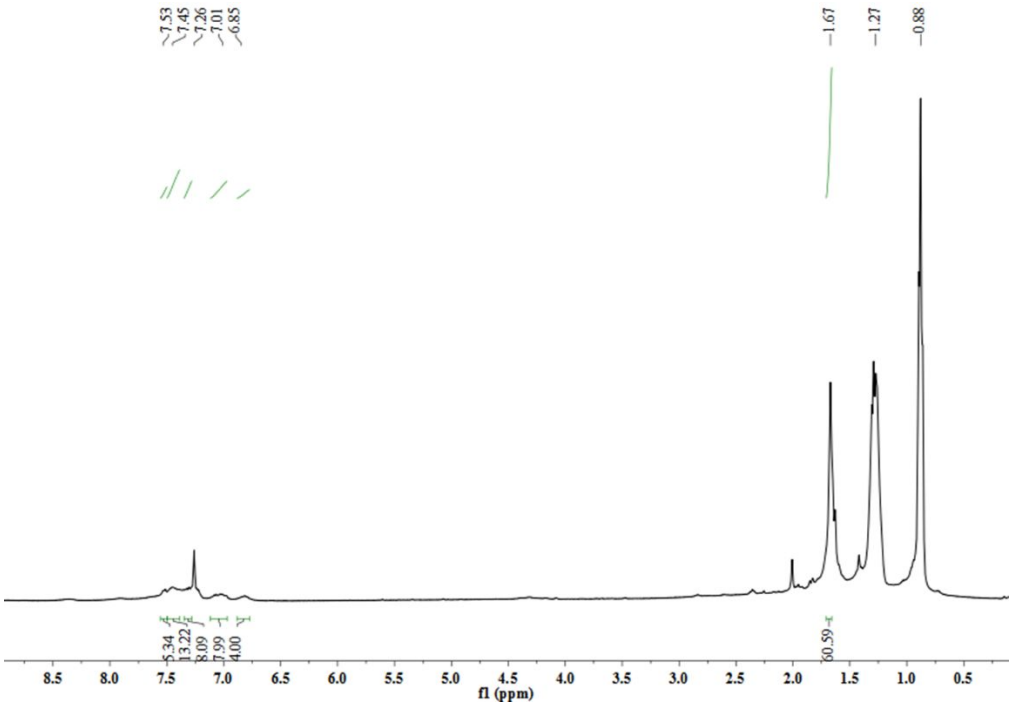

Figure S45. ^{1}H NMR (400 Hz, $CDCl_3$, ppm) of ***n*-butane⊂5a**.

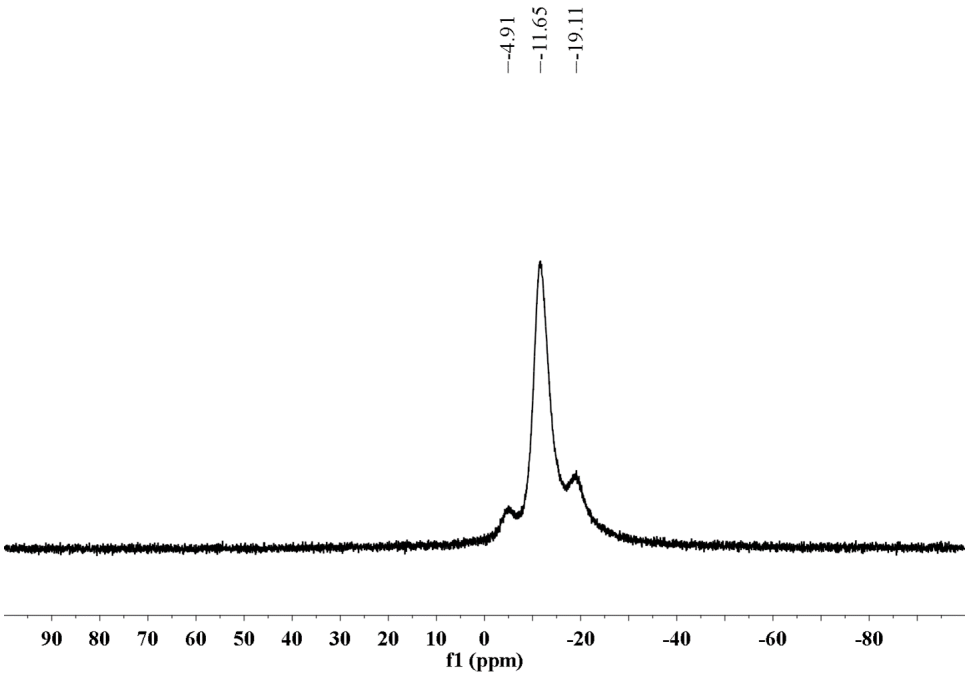

Figure S46. ^{11}B NMR (160 MHz, $CDCl_3$, ppm) of ***n*-butane⊂5a**.

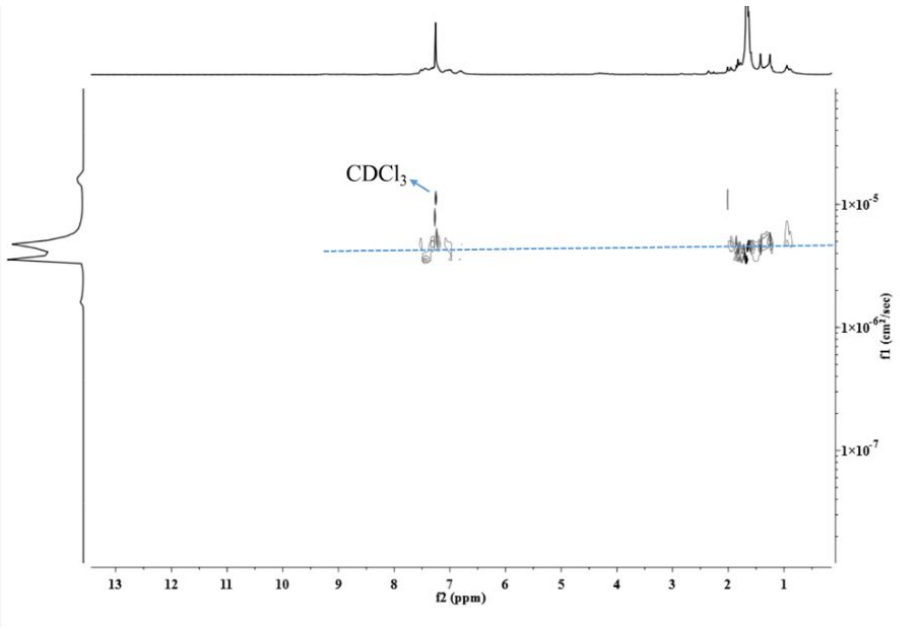

Figure S47. ^{1}H DOSY spectrum ($CDCl_3$, 400 MHz, 25 °C) of complex **5a** with *n*-butane.

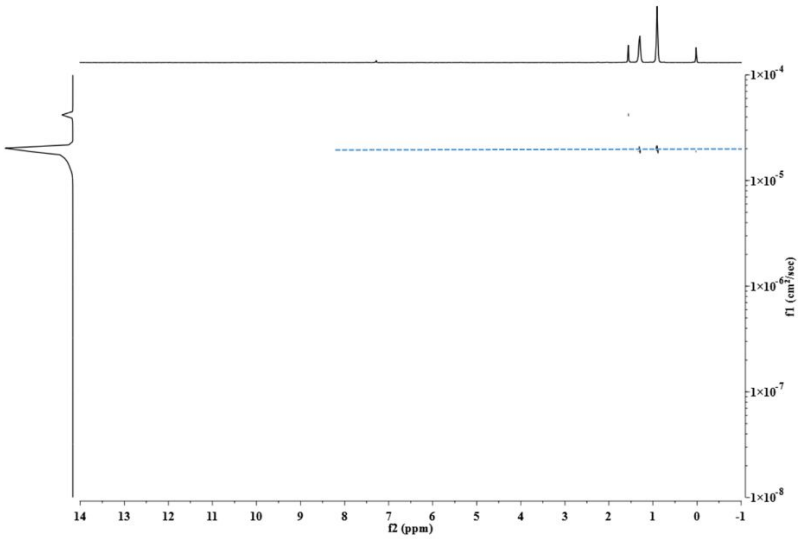

Figure S48. ^{1}H DOSY spectrum ($CDCl_3$, 400 MHz, 25 °C) of free *n*-butane.

ESI-MS spectra:

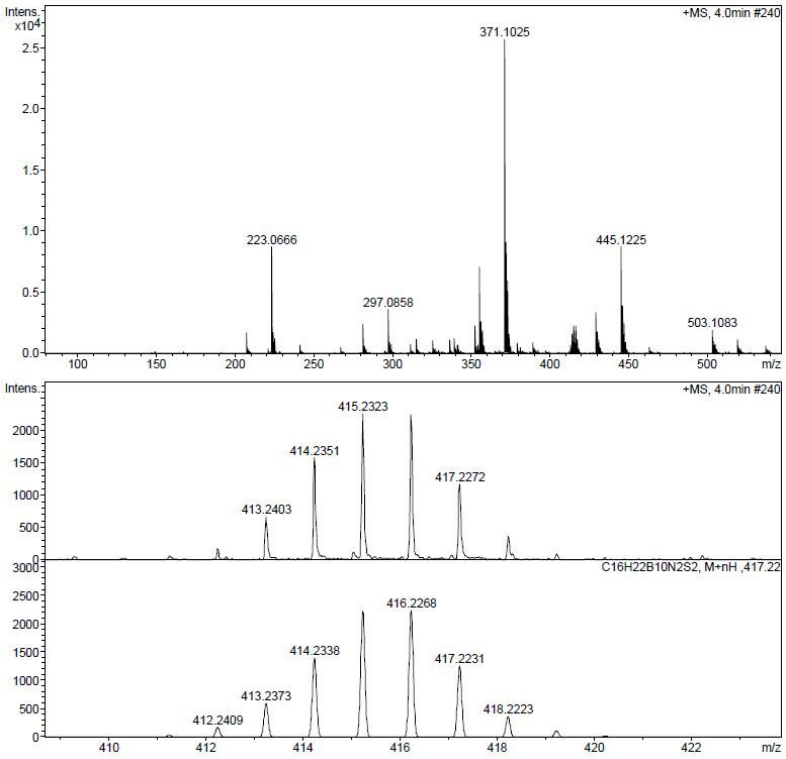

Figure S49. Experimental (top) and theoretical (bottom) ESI-MS spectra of complex **L1**.

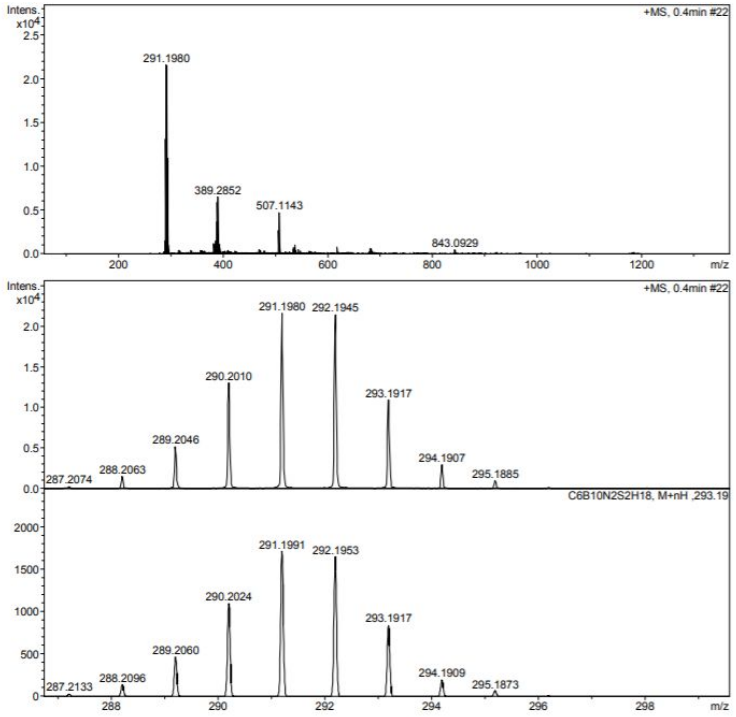

Figure S50. Experimental (top) and theoretical (bottom) ESI-MS spectra of complex **L2**.

TGA:

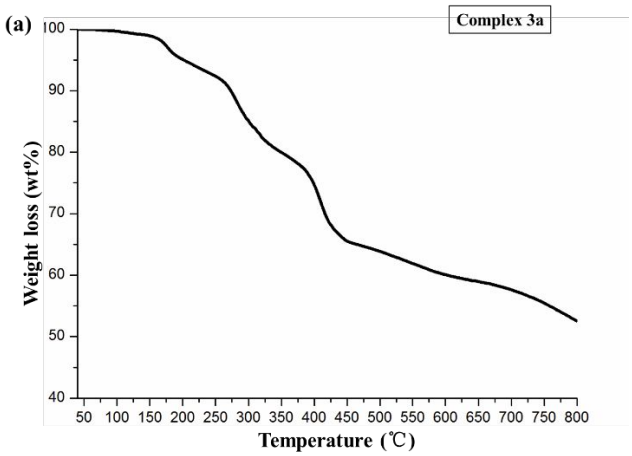
(a)
Complex 3a
Weight loss (wt%)
Temperature (℃)

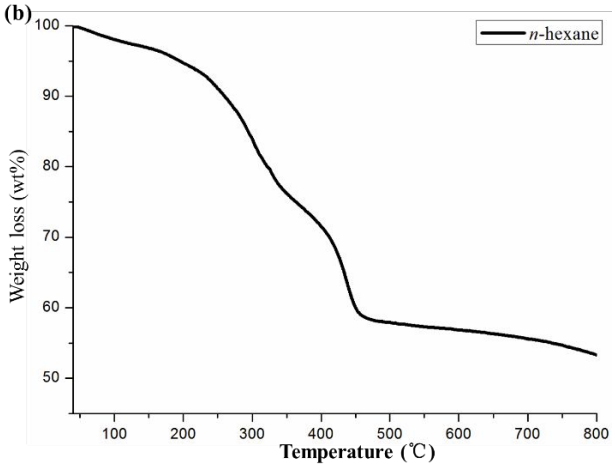
(b)
n-hexane
Weight loss (wt%)
Temperature (℃)

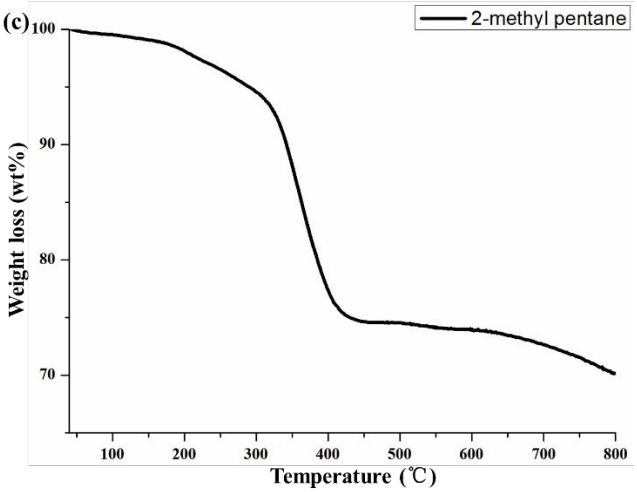
(c)
2-methyl pentane
Weight loss (wt%)
Temperature (℃)

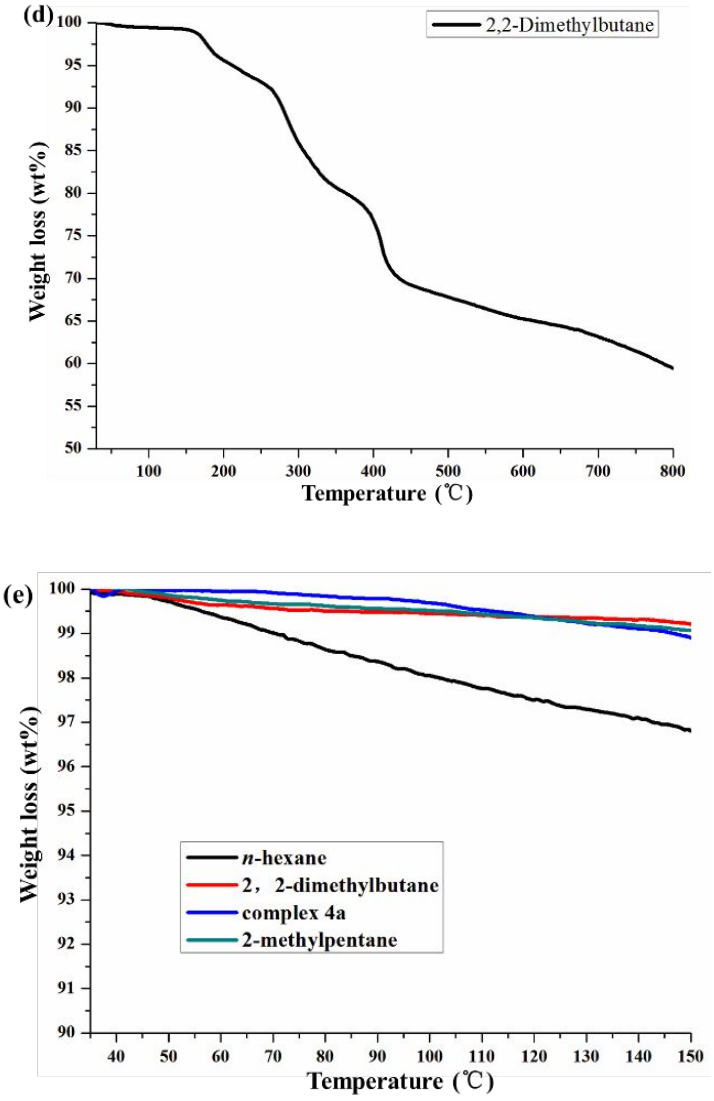

Figure S51. TGA study of (a) the complex **3a**; the complex solids prepared by exposing activated complex **3a** to hexane isomers solution: (b) *n*-hexane, (c) *2*-methylpentane and (d) *2*,*2*-dimethylbutane containing. It indicates that the complex **3a** remained stable at 140 °C. The solids immersed in *2*-methylpentane and *2*,*2*-dimethylbutane almost don't lose weight and the solids immersed in *n*-hexane lost about 3.5% weight.

IGA:

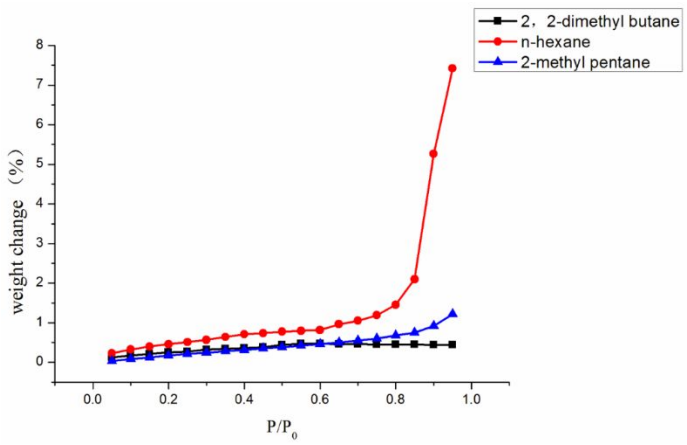

Figure S52. Adsorption profiles of *n*-hexane, *2*-methyl pentane and *2*,*2*-dimethyl butane on complex **3a** (measured by Intelligent Gravimetric Analyser at a constant temperature of 298 K). This adsorption curve indicates that the selectivity adsorption of *n*-hexane.

GC-MS:

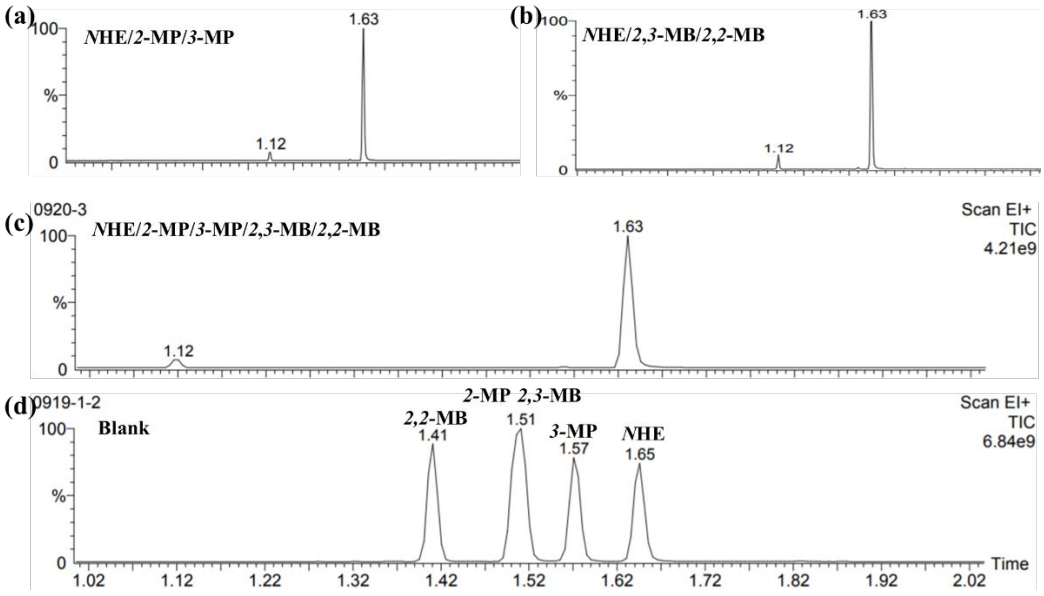

Figure S53. Mixture separation performance. Relative uptakes of *n*-hexane adsorbed in complex **3a** after absorption of the (a) *n*-hexane (N-HE), *2*-methyl pentane (2-MP) and *3*-methyl pentane (3-MP); (b) *n*-hexane (N-HE), *2*,*2*-methyl butane (*2*,*2*-MB) and *2*,*3*-methyl butane (*2*,*3*-MB); (c) N-HE, *2*-MP, *3*-MP, *2*,*2*-MB and *2*,*3*-MB equimolar mixture vapour for 24 h using head space gas chromatography. (d) The shift of the five isomers.

The Control-experiments:

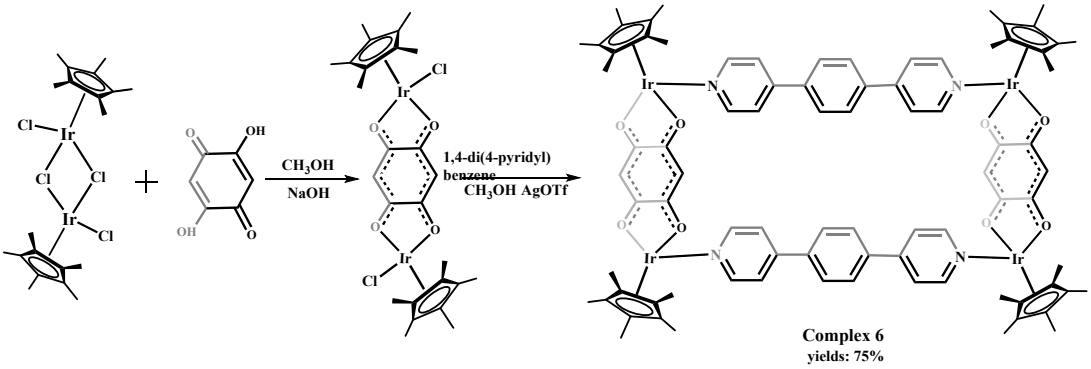

Scheme S12. Synthesis of complex **6**.

Synthesis of complex 6. $[Cp^*IrCl_2]_2$ (24 mg, 0.03 mmol) and *2,5*-Dihydroxy-*1,4*-benzoquinone (4.2 mg, 0.03mmol) were added in CH_3OH (10 ml) stirring for 10h. Then the 1,4-di(4-pyridyl) benzene (7.7 mg, 0.03 mmol) and AgOTf (31 mg, 0.12 mmol) were added to the mixture in dark at room temperature. The reaction mixture was stirred for another 24h then filtered. The filtrate was crystallized from CH_3OH/diethyl ether. Brown solids were obtained to give the complex **6**: 21 mg 75%. ^1H NMR (400 MHz; CD_3OD, ppm): δ = 1.65 (s, 60H, Cp*-H); 5.94 (s, 4H, Ar-H); 7.86 (d, 16H, Pyridine-H); 8.40 (s, 8H, Ar-H). Anal. Calcd for complex **6**: C_{88} H_{88} Ir_4 N_4 S_4 O_{20} F_{12}: C, 39.93; H, 3.35; N, 2.12. Found: C, 39.65; H, 3.09; N, 2.31.

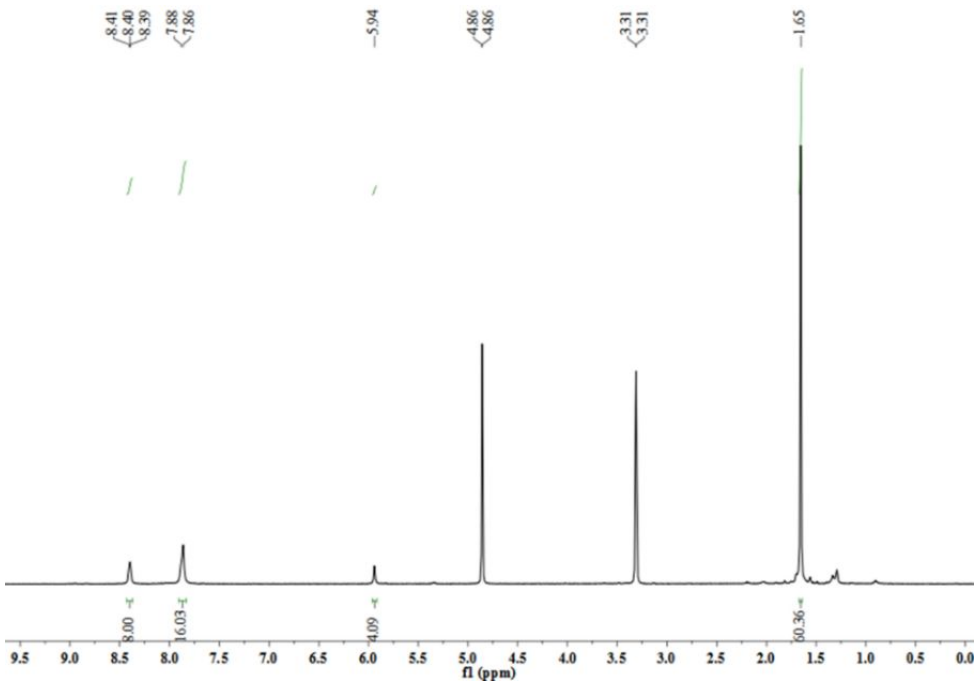

Figure S54. ^{1}H NMR (400 Hz, CD_3OD, ppm) of **6**.

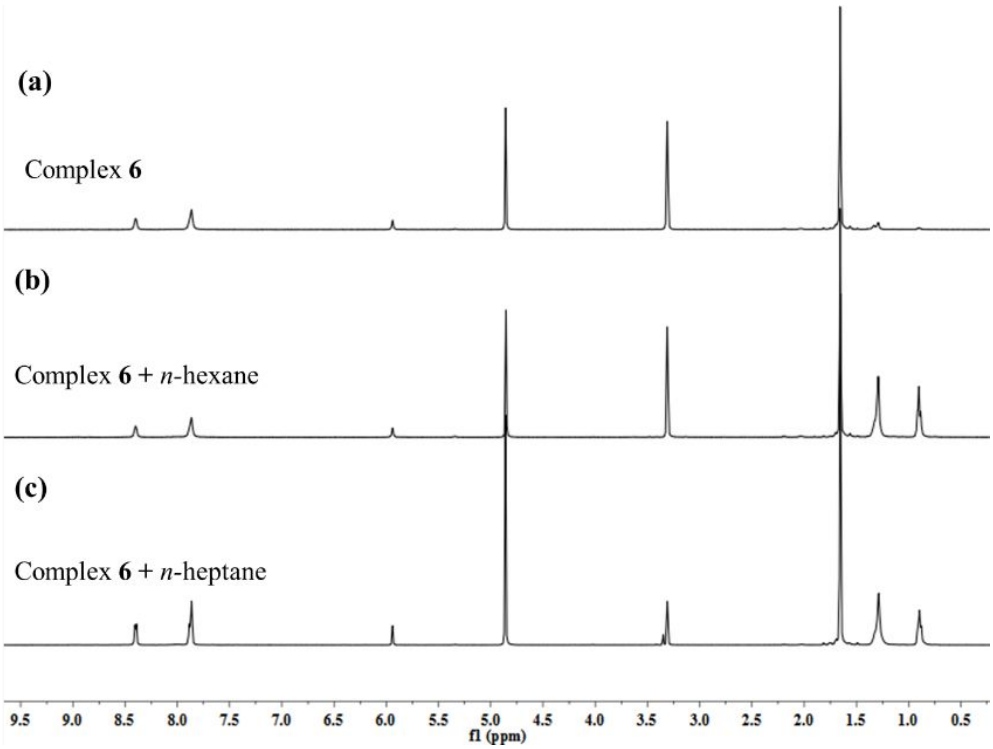

Figure S55. ^{1}H NMR spectrum (298K, 400 MHz, CD_3OD, ppm) (a) Complex **6**; (b) Complex **6** after soaking in *n*-hexane solution for 24h; (c) complex **6** after soaking in *n*-heptane solution for 24h. The proton signals don't change in the spectrum.

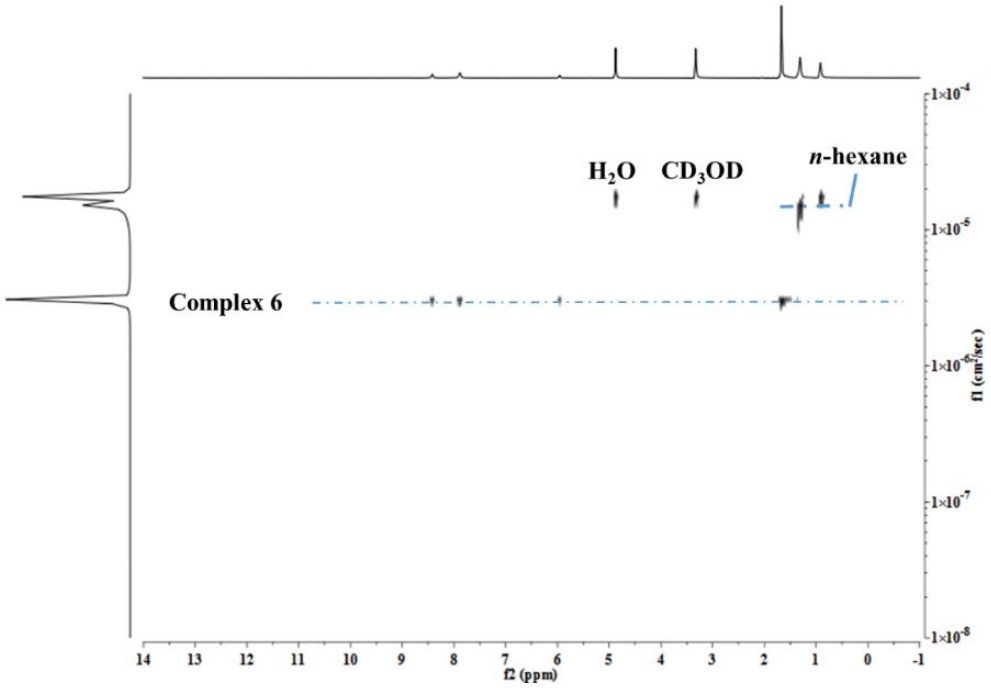

Figure S56. ^{1}H DOSY spectrum (CD_3OD, 400 MHz, 25 °C) of complex **6** with *n*-hexane.

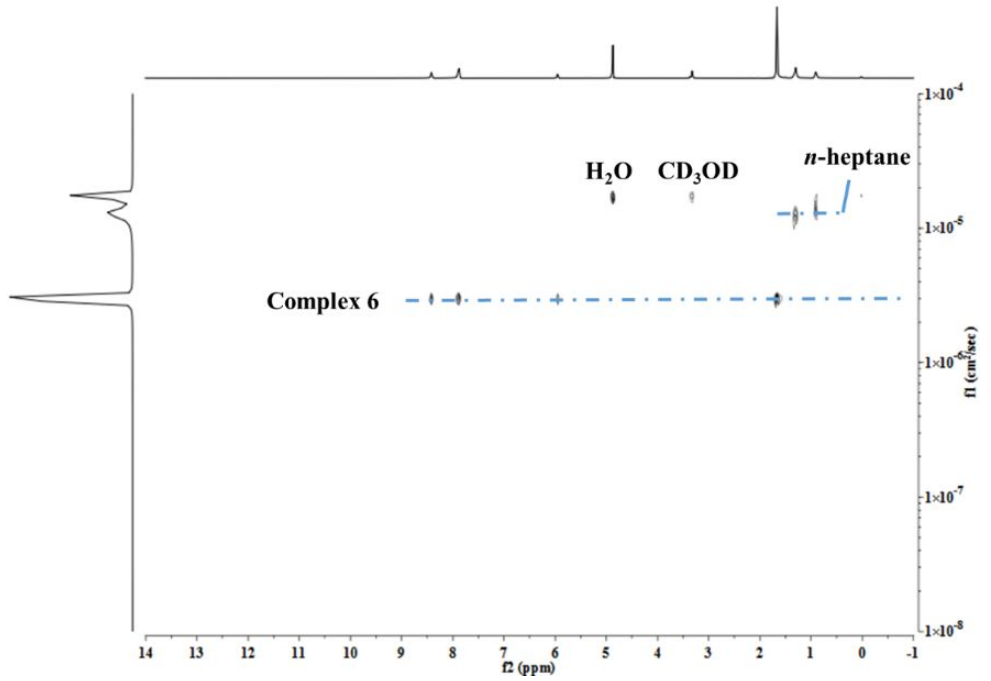

Figure S57. ^{1}H DOSY spectrum (CD_3OD, 400 MHz, 25 °C) of complex **6** with *n*-heptane.

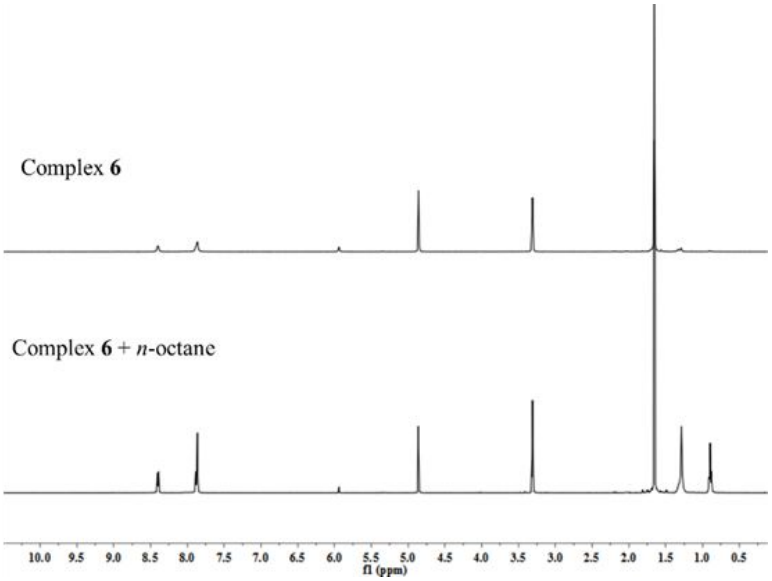

Figure S58. ^{1}H NMR spectrum (298K, 400 MHz, CD_3OD, ppm) (a) Complex **6**; (b) Complex **6** after soaking in *n*-octane solution for 24h; (c) complex **6** after soaking in *n*-octane solution for 24h. The proton signals don't change in the spectrum.

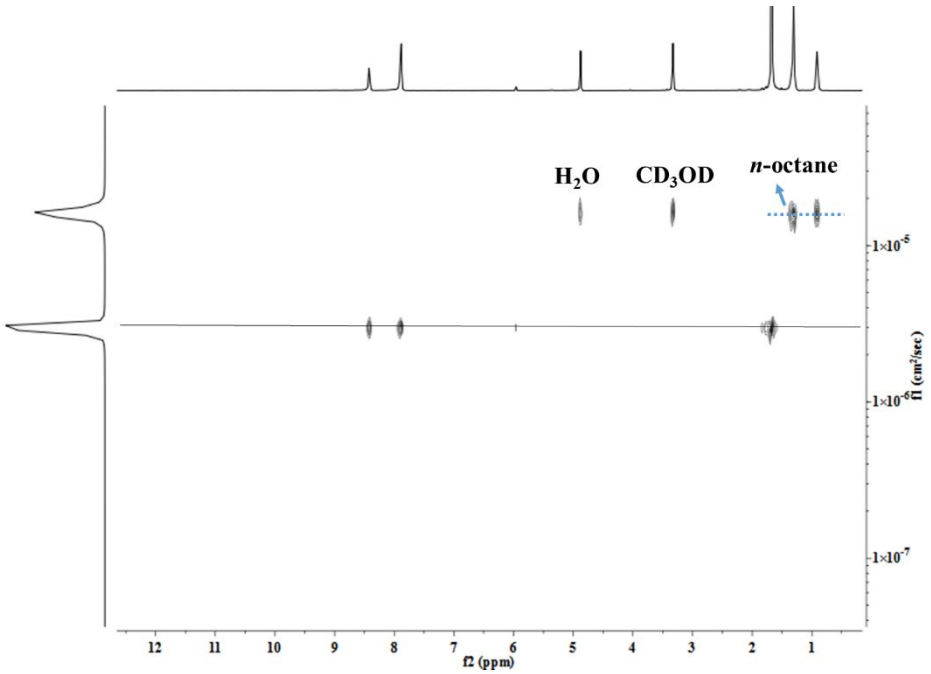

Figure S59. ^{1}H DOSY spectrum (CD_3OD, 400 MHz, 25 °C) of complex **6** with *n*-octane.

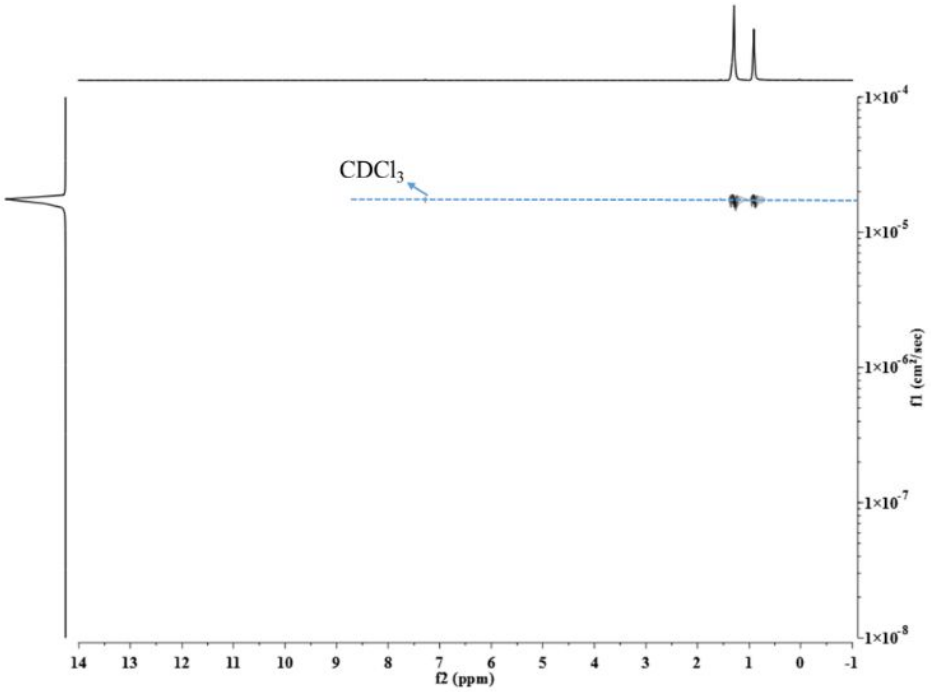

Figure S60. ^{1}H DOSY spectrum ($CDCl_3$, 400 MHz, 25 °C) of free *n*-heptane.

Crystallographic Information：

Single crystal of **L1** suitable for X-ray diffraction study was obtained at room temperature. Single crystals of **3a**, ***n*-hexane⊂3a**, **4a**, ***n*-pentane⊂4a**, ***2*-methylpentane⊂4a**, ***3*-methylpentane⊂4a**, **5b** and **6** suitable for X-ray diffraction study were obtained at low temperature. X-ray intensity data of **L1** was collected on a CCD-Bruker SMART APEX system. X-ray intensity data of the others were collected on a Bruker D8 Venture system.

In asymmetric unit of **3a**, there were disordered solvents (one diethyl ether and three water molecules) which could not be restrained properly. Therefore, SQUEEZE algorithm was used to omit them. Phenyl group of carborane ligand, benzene ring of bipyridine ligand and pentamethylcyclopentadienyl fragments (Cp* for short) were disordered and they were divided into two parts (38:62, 60:40 for phenyl group, 38:62 for benzene ring and 53:47, 58:42 for Cp*). 79 ISOR, 5 SIMU and 15 DFIX instructions were used to restrain anions, ligands and Cp* fragments so that there were 579 restraints in the data.

In asymmetric unit of complex ***n*-hexane⊂3a**, there were disordered solvent molecules (one chloroform and half of an n-hexane molecules) which could not be restrained properly. Therefore, SQUEEZE algorithm was used to omit them. One phenyl group of carborane ligand and one Cp* fragment were disordered and they were divided into two parts (65:35 for phenyl group and 63:37 for Cp* fragment). 40 ISOR, 1 FLAT, 2 SIMU and 10 DFIX instructions were used to restrain anions, ligands and Cp* fragments so that there were 325 restraints in the data.

In asymmetric unit of **4a**, there were disordered solvent molecules (one diethyl ether, half of a dichloromethane and one water molecules) which could not be restrained properly. Therefore, SQUEEZE algorithm was used to omit them. C50 and O1 were refined isotropically and other non-hydrogen atoms were refined anisotropically. 15 ISOR, 4 DELU and 15 DFIX instructions were used to restrain anions, solvents and Cp* fragments so that there were 113 restraints in the data.

In asymmetric unit of ***n*-pentane⊂4a**, there were disordered solvent molecules (two dichloromethane and one water molecules) which could not be restrained properly. Therefore, SQUEEZE algorithm was used to omit them. One phenyl group and one pentamethylcyclopentadienyl ligand (Cp* for short) were disordered and they were divided into two parts (73:27 and 70:30). 37 ISOR, 3 SIMU, 1 DELU and 15 DFIX instructions were used to restrain anions, solvents and Cp* fragments so that there were 256 restraints in the data.

In asymmetric unit of ***2*-methylpentane⊂4a**, there were disordered solvent molecules (two dichloromethane molecules) which could not be restrained properly. Therefore, SQUEEZE algorithm was used to omit them. 17 ISOR and 9 DFIX instructions were used to restrain solvents and Cp* fragments so that there were 111 restraints in the data.

In asymmetric unit of ***3*-methylpentane⊂4a**, there were disordered solvent molecules (one dichloromethane and one diethyl ether molecules) which could not be restrained properly. Therefore, SQUEEZE algorithm was used to omit them. C50 and C54 refined isotropically and other non-

hydrogen atoms were refined anisotropically. 11 ISOR, 1 SIMU and 16 DFIX instructions were used to restrain solvents and Cp* fragments so that there were 100 restraints in the data.

In asymmetric unit of **5b**, there were disordered anions and solvents (three triflate anions, one diethylether, nine acetonitrile, three methanol and three water molecules) which could not be restrained properly. Therefore, SQUEEZE algorithm was used to omit them. One metallo-angle (including Ir3 and coordinated Cp* fragment) was disordered and it was divided into two parts (69:31). 33 ISOR, 2 DELU and 8 DFIX instructions were used to restrain anion and Cp* fragments so that there were 209 restraints in the data.

In asymmetric unit of complex **6**, there were disordered solvent molecules (one diethyl ether and one methanol molecules) which could not be restrained properly. Therefore, SQUEEZE algorithm was used to omit them. One pentamethylcyclopentadienyl ligand (Cp* for short) and one diethyl ether molecule were disordered and they were divided into two parts (56:44 for Cp* and 47:53 for diethyl ether). 30 ISOR, 2 SIMU and 13 DFIX instructions were used to restrain anions, solvent molecule and Cp* fragments so that there were 265 restraints in the data.

Table S1. Crystal data and structure refinement for **L1**.

CCDC	1860025	
Empirical formula	C8 H11 B5 N S	
Formula weight	207.29	
Temperature	173(2) K	
Wavelength	0.71073 Å	
Crystal system	Monoclinic	
Space group	$P2_1/c$	
Unit cell dimensions	a = 12.2385(19) Å	a= 90°.
	b = 7.2735(11) Å	b= 106.522(2)°.
	c = 12.3850(19) Å	g = 90°.
Volume	1057.0(3) $Å^3$	
Z	4	
Density (calculated)	1.303 Mg/m^3	
Absorption coefficient	0.259 mm^{-1}	
F(000)	428	
Crystal size	0.450 x 0.360 x 0.130 mm^3	
Theta range for data collection	1.736 to 27.408°.	
Index ranges	-15<=h<=15, -5<=k<=9, -14<=l<=15	
Reflections collected	7247	
Independent reflections	2386 [R(int) = 0.0248]	
Completeness to theta = 25.242°	99.0 %	
Absorption correction	Semi-empirical from equivalents	
Max. and min. transmission	0.746 and 0.641	
Refinement method	Full-matrix least-squares on F^2	
Data / restraints / parameters	2386 / 1 / 140	
Goodness-of-fit on F^2	1.144	
Final R indices [I>2sigma(I)]	R1 = 0.0441, wR2 = 0.1173	
R indices (all data)	R1 = 0.0528, wR2 = 0.1217	
Extinction coefficient	n/a	
Largest diff. peak and hole	0.343 and -0.328 $e.Å^{-3}$	

Table S2. Crystal data and structure refinement for **3a**.

CCDC	1979011	
Empirical formula	C112 H152 B20 Ir4 N8 O8 S4	
Formula weight	2851.65	
Temperature	173(2) K	
Wavelength	1.34138 Å	
Crystal system	Orthorhombic	
Space group	Pbca	
Unit cell dimensions	a = 22.3072(9) Å	a= 90°.
	b = 17.7179(8) Å	b= 90°.
	c = 30.6044(14) Å	g = 90°.
Volume	12096.0(9) $Å^3$	
Z	4	
Density (calculated)	1.566 Mg/m^3	
Absorption coefficient	6.231 mm^{-1}	
F(000)	5664	
Crystal size	0.230 x 0.210 x 0.120 mm^3	
Theta range for data collection	3.043 to 54.971°.	
Index ranges	-27<=h<=25, -20<=k<=21, -33<=l<=37	
Reflections collected	61627	
Independent reflections	11494 [R(int) = 0.0820]	
Completeness to theta = 53.594°	99.9 %	
Absorption correction	Semi-empirical from equivalents	
Max. and min. transmission	0.751 and 0.524	
Refinement method	Full-matrix least-squares on F^2	
Data / restraints / parameters	11494 / 579 / 859	
Goodness-of-fit on F^2	1.068	
Final R indices [I>2sigma(I)]	R1 = 0.0730, wR2 = 0.1754	
R indices (all data)	R1 = 0.0926, wR2 = 0.1859	
Extinction coefficient	n/a	
Largest diff. peak and hole	1.876 and -1.370 $e.Å^{-3}$	

Table S3. Crystal data and structure refinement for ***n*-hexane⊂3a**.

CCDC	1860033	
Empirical formula	C126 H166 B20 Cl12 Ir4 N8 S4	
Formula weight	3331.30	
Temperature	173(2) K	
Wavelength	1.34138 Å	
Crystal system	Triclinic	
Space group	P-1	
Unit cell dimensions	a = 12.9434(5) Å	a= 78.963(2)°.
	b = 13.4088(5) Å	b= 74.853(2)°.
	c = 22.5389(9) Å	g = 71.967(2)°.
Volume	3564.2(2) $Å^3$	
Z	1	
Density (calculated)	1.552 Mg/m^3	
Absorption coefficient	6.667 mm^{-1}	
F(000)	1654	
Crystal size	0.200 x 0.070 x 0.010 mm^3	
Theta range for data collection	3.702 to 56.056°.	
Index ranges	-15<=h<=15, -16<=k<=16, -27<=l<=27	
Reflections collected	40238	
Independent reflections	13981 [R(int) = 0.0873]	
Completeness to theta = 53.594°	99.8 %	
Absorption correction	Semi-empirical from equivalents	
Max. and min. transmission	0.657 and 0.416	
Refinement method	Full-matrix least-squares on F^2	
Data / restraints / parameters	13981 / 325 / 858	
Goodness-of-fit on F^2	1.043	
Final R indices [I>2sigma(I)]	R1 = 0.0603, wR2 = 0.1475	
R indices (all data)	R1 = 0.0946, wR2 = 0.1634	
Extinction coefficient	n/a	
Largest diff. peak and hole	2.685 and -2.243 e.$Å^{-3}$	

Table S4. Crystal data and structure refinement for **4a**.

CCDC	1979012	
Empirical formula	C109 H152 B20 Cl2 Ir4 N8 O5 S4	
Formula weight	2838.52	
Temperature	173(2) K	
Wavelength	1.34138 Å	
Crystal system	Monoclinic	
Space group	$P2_1/c$	
Unit cell dimensions	a = 16.1210(12) Å	a= 90°.
	b = 20.2886(17) Å	b= 101.203(4)°.
	c = 19.1144(15) Å	g = 90°.
Volume	6132.7(8) $Å^3$	
Z	2	
Density (calculated)	1.537 Mg/m^3	
Absorption coefficient	6.392 mm^{-1}	
F(000)	2816	
Crystal size	0.120 x 0.110 x 0.100 mm^3	
Theta range for data collection	3.431 to 56.500°.	
Index ranges	-17<=h<=20, -25<=k<=17, -23<=l<=21	
Reflections collected	55959	
Independent reflections	12318 [R(int) = 0.1380]	
Completeness to theta = 53.594°	99.7 %	
Absorption correction	Semi-empirical from equivalents	
Max. and min. transmission	0.580 and 0.379	
Refinement method	Full-matrix least-squares on F^2	
Data / restraints / parameters	12318 / 113 / 639	
Goodness-of-fit on F^2	1.025	
Final R indices [I>2sigma(I)]	R1 = 0.1127, wR2 = 0.2765	
R indices (all data)	R1 = 0.1665, wR2 = 0.3300	
Extinction coefficient	n/a	
Largest diff. peak and hole	2.708 and -1.538 $e.Å^{-3}$	

Table S5. Crystal data and structure refinement for ***n*-pentane⊂4a**.

CCDC	1979017	
Empirical formula	C103 H140 B20 Cl4 Ir4 N8 O2 S4	
Formula weight	2777.26	
Temperature	173(2) K	
Wavelength	1.34138 Å	
Crystal system	Monoclinic	
Space group	$P2_1/c$	
Unit cell dimensions	a = 16.1658(6) Å	a= 90°.
	b = 20.1310(8) Å	b= 101.290(2)°.
	c = 19.0507(8) Å	g = 90°.
Volume	6079.8(4) $Å^3$	
Z	2	
Density (calculated)	1.517 Mg/m^3	
Absorption coefficient	6.691 mm^{-1}	
F(000)	2740	
Crystal size	0.140 x 0.120 x 0.110 mm^3	
Theta range for data collection	3.087 to 56.500°.	
Index ranges	-18<=h<=20, -19<=k<=25, -23<=l<=23	
Reflections collected	45118	
Independent reflections	12204 [R(int) = 0.0757]	
Completeness to theta = 53.594°	99.8 %	
Absorption correction	Semi-empirical from equivalents	
Max. and min. transmission	0.751 and 0.539	
Refinement method	Full-matrix least-squares on F^2	
Data / restraints / parameters	12204 / 256 / 765	
Goodness-of-fit on F^2	1.038	
Final R indices [I>2sigma(I)]	R1 = 0.0770, wR2 = 0.2225	
R indices (all data)	R1 = 0.1160, wR2 = 0.2569	
Extinction coefficient	n/a	
Largest diff. peak and hole	2.295 and -2.071 $e.Å^{-3}$	

Table S6. Crystal data and structure refinement for ***2*-methylpentane⊂4a**.

CCDC	1979016	
Empirical formula	C106 H138 B20 Cl8 Ir4 N8 S4	
Formula weight	2921.08	
Temperature	172.99 K	
Wavelength	1.34138 Å	
Crystal system	Monoclinic	
Space group	P 1 21/c 1	
Unit cell dimensions	a = 16.1760(7) Å	a= 90°.
	b = 20.1918(9) Å	b= 101.191(2)°.
	c = 19.1978(8) Å	g = 90°.
Volume	6151.2(5) $Å^3$	
Z	2	
Density (calculated)	1.577 Mg/m^3	
Absorption coefficient	7.378 mm^{-1}	
F(000)	2876	
Crystal size	0.23 x 0.21 x 0.19 mm^3	
Theta range for data collection	3.081 to 56.499°.	
Index ranges	-20<=h<=20, -21<=k<=25, -23<=l<=23	
Reflections collected	56534	
Independent reflections	12376 [R(int) = 0.0627]	
Completeness to theta = 53.594°	99.9 %	
Absorption correction	Semi-empirical from equivalents	
Max. and min. transmission	0.7512 and 0.4715	
Refinement method	Full-matrix least-squares on F^2	
Data / restraints / parameters	12376 / 111 / 662	
Goodness-of-fit on F^2	1.034	
Final R indices [I>2sigma(I)]	R1 = 0.0639, wR2 = 0.1847	
R indices (all data)	R1 = 0.0731, wR2 = 0.1952	
Extinction coefficient	n/a	
Largest diff. peak and hole	4.660 and -1.690 $e.Å^{-3}$	

Table S7. Crystal data and structure refinement for ***3*-methylpentane⊂4a**.

CCDC	1979015	
Empirical formula	C112 H154 B20 Cl4 Ir4 N8 O2 S4	
Formula weight	2899.46	
Temperature	173(2) K	
Wavelength	1.34138 Å	
Crystal system	Monoclinic	
Space group	$P2_1/c$	
Unit cell dimensions	a = 16.0980(5) Å	a= 90°.
	b = 20.2517(7) Å	b= 101.186(2)°.
	c = 19.1809(6) Å	g = 90°.
Volume	6134.4(3) $Å^3$	
Z	2	
Density (calculated)	1.570 Mg/m^3	
Absorption coefficient	6.649 mm^{-1}	
F(000)	2876	
Crystal size	0.150 x 0.130 x 0.110 mm^3	
Theta range for data collection	4.088 to 56.500°.	
Index ranges	-20<=h<=20, -25<=k<=20, -23<=l<=23	
Reflections collected	46685	
Independent reflections	12318 [R(int) = 0.1167]	
Completeness to theta = 53.594°	99.8 %	
Absorption correction	Semi-empirical from equivalents	
Max. and min. transmission	0.751 and 0.520	
Refinement method	Full-matrix least-squares on F^2	
Data / restraints / parameters	12318 / 100 / 649	
Goodness-of-fit on F^2	0.950	
Final R indices [I>2sigma(I)]	R1 = 0.0676, wR2 = 0.1653	
R indices (all data)	R1 = 0.1466, wR2 = 0.2050	
Extinction coefficient	n/a	
Largest diff. peak and hole	1.606 and -1.055 $e.Å^{-3}$	

Table **S8**. Crystal data and structure refinement for **5b**.

CCDC	1979014	
Empirical formula	C101 H163 B20 F12 Ir4 N17 O19 S8	
Formula weight	3388.95	
Temperature	173(2) K	
Wavelength	1.34138 Å	
Crystal system	Monoclinic	
Space group	C2/c	
Unit cell dimensions	a = 30.973(2) Å	a= 90°.
	b = 36.1780(18) Å	b= 118.943(5)°.
	c = 26.393(2) Å	g = 90°.
Volume	25880(3) $Å^3$	
Z	8	
Density (calculated)	1.740 Mg/m^3	
Absorption coefficient	6.427 mm^{-1}	
F(000)	13472	
Crystal size	0.400 x 0.240 x 0.160 mm^3	
Theta range for data collection	2.699 to 58.000°.	
Index ranges	-39<=h<=39, -43<=k<=45, -33<=l<=33	
Reflections collected	290568	
Independent reflections	27356 [R(int) = 0.0537]	
Completeness to theta = 53.594°	99.8 %	
Absorption correction	Semi-empirical from equivalents	
Max. and min. transmission	0.751 and 0.301	
Refinement method	Full-matrix least-squares on F^2	
Data / restraints / parameters	27356 / 209 / 1151	
Goodness-of-fit on F^2	1.010	
Final R indices [I>2sigma(I)]	R1 = 0.0776, wR2 = 0.2210	
R indices (all data)	R1 = 0.0828, wR2 = 0.2266	
Extinction coefficient	n/a	
Largest diff. peak and hole	10.365 and -2.898 e.$Å^{-3}$	

Table S9. Crystal data and structure refinement for complex **6**.

CCDC	1979013	
Empirical formula	C106 H136 F12 Ir4 N4 O26 S4	
Formula weight	3007.22	
Temperature	143(2) K	
Wavelength	1.34138 Å	
Crystal system	Orthorhombic	
Space group	Pbca	
Unit cell dimensions	a = 21.999(4) Å	a= 90°.
	b = 18.835(4) Å	b= 90°.
	c = 27.602(6) Å	g = 90°.
Volume	11437(4) $Å^3$	
Z	4	
Density (calculated)	1.747 Mg/m^3	
Absorption coefficient	6.799 mm^{-1}	
F(000)	5952	
Crystal size	0.230 x 0.190 x 0.180 mm^3	
Theta range for data collection	3.872 to 59.999°.	
Index ranges	-26<=h<=28, -24<=k<=23, -35<=l<=35	
Reflections collected	171034	
Independent reflections	12788 [R(int) = 0.0483]	
Completeness to theta = 53.594°	98.8 %	
Absorption correction	Semi-empirical from equivalents	
Max. and min. transmission	0.754 and 0.445	
Refinement method	Full-matrix least-squares on F^2	
Data / restraints / parameters	12788 / 265 / 742	
Goodness-of-fit on F^2	1.035	
Final R indices [I>2sigma(I)]	R1 = 0.0422, wR2 = 0.1206	
R indices (all data)	R1 = 0.0439, wR2 = 0.1226	
Extinction coefficient	n/a	
Largest diff. peak and hole	1.568 and -1.274 $e.Å^{-3}$	

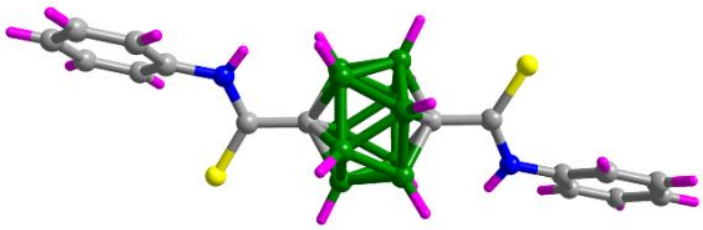

Figure S61. Crystallographically derived molecular structure of **Ligand 1**. Color code: S, yellow; N, blue; C, grey; B, green; H, pink.

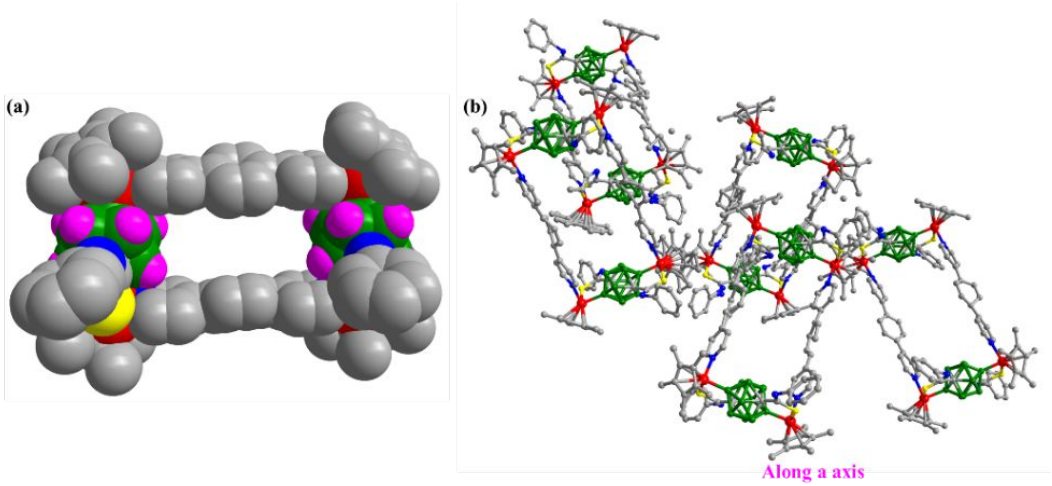

Figure S62. Crystallographically derived molecular structure of complex **3a**: (a) the space-filling mode; (b) the packing mode (Along a axis). (The H atoms except for carborane cage have been omitted for clarity). Color code: Ir, red; S, yellow; N, blue; C, grey; B, green.

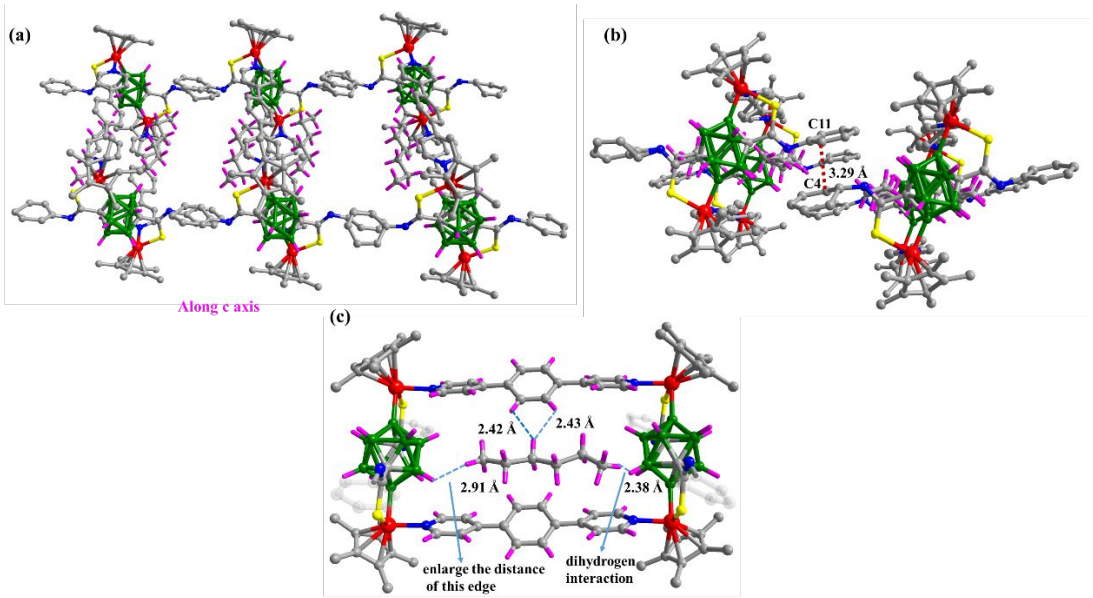

Figure S63. Crystallographically derived molecular structure of complex ***n*-hexane⊂3a**: (a) the packing mode (Along c axis); (b) the C···C interaction between every two metallacycles; (c) the H···H distance between the *n*-hexane and DPB. (The H atoms of Cp* and the benzene of Ligand **1** have been omitted for clarity). Color code: Ir, red; S, yellow; N, blue; C, grey; B, green; H, pink.

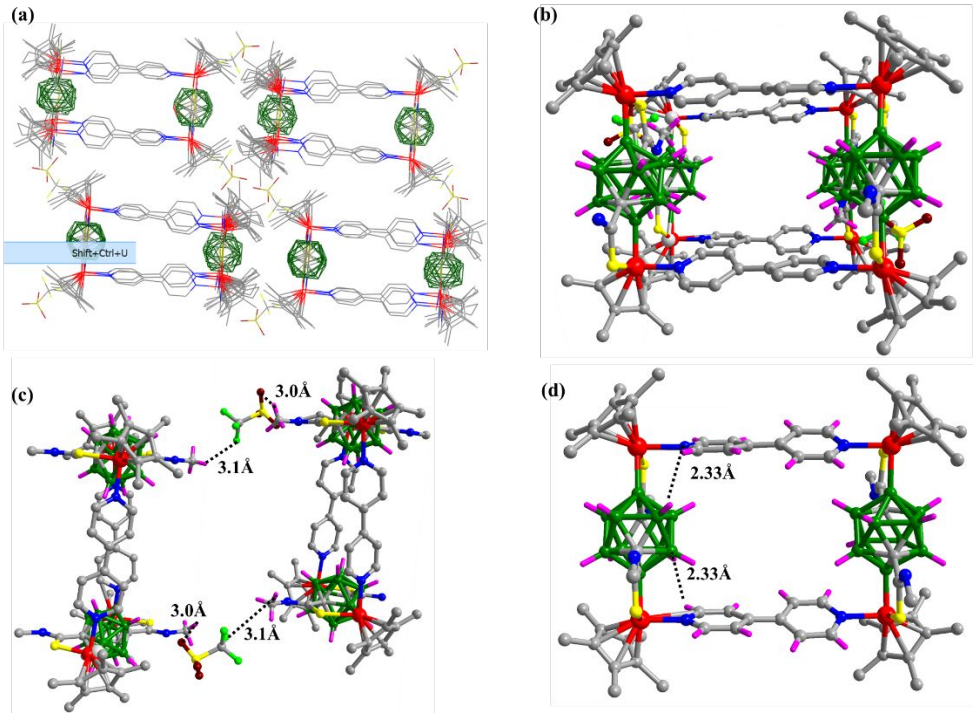

Figure S64. Crystallographically derived molecular structure of complex **5b**: (a) the packing mode to form a one-dimensional channel (Along b axis); (b) the cavity of the complex **5b**; (c) the C-H···F and C-H…O interactions between every two metallacycles; (d) C-H···H-B dihydrogen interactions of **5b**. (The H atoms have been omitted for clarity except for carborane cage). Color code: Ir, red; S, yellow; N, blue; C, grey; B, green; H, pink; O dark red.

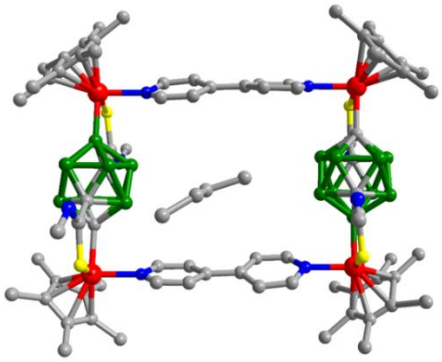

Figure S65. The data obtained for ***n*-butane⊂5b** was of poor resolution, hence a full structure will not be presented. Because of the degraded single crystallinity of the samples, as commonly encountered in similar systems[7], the SCXRD data are not of sufficient quality to determine the precise positions of the hydrogen atoms, especially for the labile guest molecules. Nevertheless, the adsorbed C4 hydrocarbon molecules could be observed inside **5b**, with clearly distinguishable molecular conformations.

DFT Calculation details:

All the calculations were performed with the B97D3 density functional method[2] using the Gaussian 09 software package.[3] The empirical long-range correction of Grimme et al was used for the B97 functional.[4] The basis sets used are: the aug-cc-pVDZ-PP pseudo potential basis set [5,6] for Ir and the 6-31G(d,p) basis set [7,8] for the other atoms.

	n-hexane	3-methylpentane	2,2-dimethylbutane
Binding energy (kcal/mol)	-36.5	-29.6	-24.7

Table S10. Binding energy of the hexane isomers with the complex **3a**.

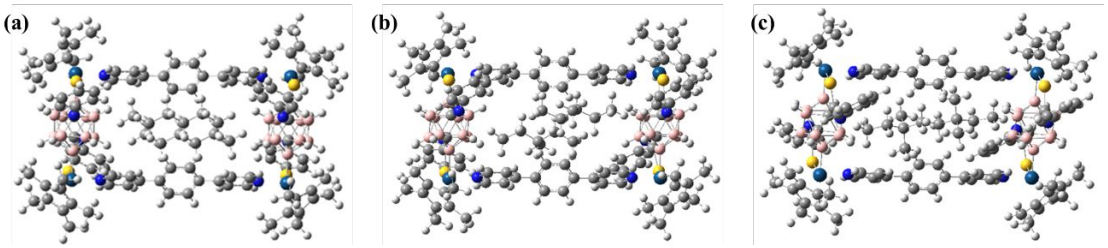

Figure S66. The DFT-D optimized *n*-hexane (a), 3-methylpentane (b) and 2,2-dimethylbutane (c) adsorption configuration in complex **3a**.

Reference:

1. White, C.; Yates, A.; Maitlis, P. M. *Inorg. Synth.* **1992**, 29, 228.
2. Chai, J.-D.; Head-Gordon, M. *Phys. Chem. Chem. Phys.* **2008**, 10, 6615.
3. Gaussian 09, Revision A.02, Frisch, M. J.; Trucks, G. W.; Schlegel, H. B.; Scuseria, G. E.; Robb, M. A.; Cheeseman, J. R.; Scalmani, G.; Barone, V.; Mennucci, B.; Petersson, G. A.; Nakatsuji, H.; Caricato, M.; Li, X.; Hratchian, H. P.; Izmaylov, A. F.; Bloino, J.; Zheng, G.; Sonnenberg, J. L.; Hada, M.; Ehara, M.; Toyota, K.; Fukuda, R.; Hasegawa, J.; Ishida, M.; Nakajima, T.; Honda, Y.; Kitao, O.; Nakai, H.; Vreven, T.; Montgomery, J. A. Jr.; Peralta, J. E.; Ogliaro, F.; Bearpark, M.; Heyd, J. J.; Brothers, E.; Kudin, K. N.; Staroverov, V. N.; Kobayashi, R.; Normand, J.; Raghavachari, K.; Rendell, A.; Burant, J. C.; Iyengar, S. S.; Tomasi, J.; Cossi, M.; Rega, N.; Millam, J. M.; Klene, M.; Knox, J. E.; Cross, J. B.; Bakken, V.; Adamo, C.; Jaramillo, J.; Gomperts, R.; Stratmann, R. E.; Yazyev, O.; Austin, A. J.; Cammi, R.; Pomelli, C.; Ochterski, J. W.; Martin, R. L.; Morokuma, K.; Zakrzewski, V. G.; Voth, G. A.; Salvador, P.; Dannenberg, J. J.; Dapprich, S.; Daniels, A. D.; Farkas, O.; Foresman, J. B.; Ortiz, J. V.; Cioslowski, J.; Fox, D. J. Gaussian, Inc., Wallingford CT, 2009.
4. Grimme, S.; Antony, J.; Ehrlich, S.; Krieg, H. J. *Chem. Phys.* **2010**, 132, 154104.
5. Andrae, D.; Haeussermann, U.; Dolg, M.; Stoll, H.; Preuss, H. *Theor. Chem. Acc.* **1990**, 77, 123.
6. Hariharan, P. C.; Pople, J. A. *Theoret. Chimica Acta* **1973**, 28, 213.
7. McLean, A. D.; Chandler, G. S. *J. Chem. Phys.* **1980**,72, 5639. (c) Krishnan, R.; Binkley, J. S.; Seeger, R.; Pople, J. A. *J. Chem. Phys.* **1980**, 72, 650.
8. Zhang, J. P.; Liao, P. Q.; Zhou, H. L.; Lin, R. B.; Chen, X. M. *Chem. Soc. Rev.* **2014**, 43, 5789.